Title: New Insights into Strong Gravity from Accreting Black Holes

Speakers: Prashant Kocherlakota

Series: Strong Gravity

Date: March 14, 2024 - 1:00 PM

URL: https://pirsa.org/24030113

Abstract: Recent horizon-scale images of Messier 87* and Sagittarius A* have been used to demonstrate that their spacetimes are well-described by the Kerr metric. The latter is a solution to the vacuum Einstein equations of general relativity, and is used to describe spinning black holes. While of fundamental importance, it has undesirable features such as a spacetime singularity or a Cauchy horizon. To find phenomenological resolutions of such features, using observations, studies of astrophysical processes in non-Kerr spacetimes have recently gained prominence. We will begin by briefly reviewing the current status of observational constraints on such alternatives. We will then demonstrate how future observations of the "photon ring" can grant access to new observables that will refine our physical understanding of strong-gravity. We will end by sketching how, using state-of-the-art numerical simulations, the energetics of relativistic outflows (jets) is universally described by a simple electromagnetic Penrose process (the Blandford-Znajek mechanism).

Zoom link TBA

New Insights into Strong Gravity *from Accreting Black Holes*

Prashant Kocherlakota

Black Hole Initiative at Harvard University
Center for Astrophysics | Harvard & Smithsonian

Event Horizon Telescope Collaboration

PI Strong Gravity Seminar
14th Mar. 2024

Based on:

[1] Kocherlakota, Rezzolla, Roy, Wielgus [2307.16841, 2403.tonight]
[2] Kocherlakota, Narayan, Chatterjee, Cruz-Osorio, Mizuno [2307.15140]
[3] Chatterjee, Kocherlakota, Younsi, Narayan [2310.20040]
[4] Chatterjee, Younsi, Kocherlakota, Narayan [2310.20043]

BLACK HOLE INITIATIVE HARVARD UNIVERSITY
CENTER FOR ASTROPHYSICS HARVARD & SMITHSONIAN
NSF U.S. National Science Foundation
JOHN TEMPLETON FOUNDATION
GORDON AND BETTY MOORE FOUNDATION

Outline

[I] Measuring spacetime using black hole (BH) imaging: Current Status & Future Prospects

Kocherlakota, Rezzolla, Roy, Wielgus, 2024a, b

We have now constructed a library of simulations that realistically model hot accretion onto *non-Kerr* BHs

Chatterjee et al., 2023 a,b

[II] Observable differences between simulated images of Kerr and non-Kerr BHs

Accreting BHs can produce relativistic outflows or jets

Hubble Space Telescope, 1998

[III] Jet power of a non-Kerr BH

The Era of Strong Gravity Observations

Consistency with General Relativity (GR)

Deeper dive into strong-field gravity

Observation of Gravitational Waves from a Binary Black Hole Merger

B. P. Abbott *et al.**
(LIGO Scientific Collaboration and Virgo Collaboration)
(Received 21 January 2016; published 11 February 2016)

On September 14, 2015 at 09:50:45 UTC the two detectors of the Laser Interferometer Gravitational-Wave Observatory simultaneously observed a transient gravitational-wave signal. The signal sweeps upwards in frequency from 35 to 250 Hz with a peak gravitational-wave strain of 1.0×10^{-21}. It matches the waveform predicted by general relativity for the inspiral and merger of a pair of black holes and the ringdown of the resulting single black hole. The signal was observed with a matched-filter signal-to-noise ratio of 24 and a false alarm rate estimated to be less than 1 event per 203 000 years, equivalent to a significance greater than 5.1σ. The source lies at a luminosity distance of 410^{+160}_{-180} Mpc corresponding to a redshift $z = 0.09^{+0.03}_{-0.04}$. In the source frame, the initial black hole masses are $36^{+5}_{-4} M_\odot$ and $29^{+4}_{-4} M_\odot$, and the final black hole mass is $62^{+4}_{-4} M_\odot$, with $3.0^{+0.5}_{-0.5} M_\odot c^2$ radiated in gravitational waves. All uncertainties define 90% credible intervals. These observations demonstrate the existence of binary stellar-mass black hole systems. This is the first direct detection of gravitational waves and the first observation of a binary black hole merger.

DOI: 10.1103/PhysRevLett.116.061102

I. INTRODUCTION

In 1916, the year after the final formulation of the field equations of general relativity, Albert Einstein predicted the existence of gravitational waves. He found that the linearized weak-field equations had wave solutions: transverse waves of spatial strain that travel at the speed of light, generated by time variations of the mass quadrupole moment of the source [1,2]. Einstein understood that gravitational-wave amplitudes would be remarkably small; moreover, until the Chapel Hill conference in

The discovery of the binary pulsar system PSR B1913+16 by Hulse and Taylor [20] and subsequent observations of its energy loss by Taylor and Weisberg [21] demonstrated the existence of gravitational waves. This discovery, along with emerging astrophysical understanding [22], led to the recognition that direct observations of the amplitude and phase of gravitational waves would enable studies of additional relativistic systems and provide new tests of general relativity, especially in the dynamic strong-field regime.

Abbott et al. (LIGO, Virgo), 2016

First M87 Event Horizon Telescope Results. I. The Shadow of the Supermassive Black Hole

The Event Horizon Telescope Collaboration
(See the end matter for the full list of authors.)
Received 2019 March 1; revised 2019 March 12; accepted 2019 March 12; published 2019 April 10

Abstract

When surrounded by a transparent emission region, black holes are expected to reveal a dark shadow caused by gravitational light bending and photon capture at the event horizon. To image and study this phenomenon, we have assembled the Event Horizon Telescope, a global very long baseline interferometry array observing at a wavelength of 1.3 mm. This allows us to reconstruct event-horizon-scale images of the supermassive black hole candidate in the center of the giant elliptical galaxy M87. We have resolved the central compact radio source as an asymmetric bright emission ring with a diameter of $42 \pm 3\ \mu$as, which is circular and encompasses a central depression in brightness with a flux ratio $\gtrsim 10:1$. The emission ring is recovered using different calibration and imaging schemes, with its diameter and width remaining stable over four different observations carried out in different days. Overall, the observed image is consistent with expectations for the shadow of a Kerr black hole as predicted by general relativity. The asymmetry in brightness in the ring can be explained in terms of relativistic beaming of the emission from a plasma rotating close to the speed of light around a black hole. We compare our images to an extensive library of ray-traced general-relativistic magnetohydrodynamic simulations of black holes and derive a central mass of $M = (6.5 \pm 0.7) \times 10^9 M_\odot$. Our radio-wave observations thus provide powerful evidence for the presence of supermassive black holes in centers of galaxies and as the central engines of active galactic nuclei. They also present a new tool to explore gravity in its most extreme limit and on a mass scale that was so far not accessible.

EHTC M87* Paper I, 2019

The Larger Context: Gravity Experiments across Scales

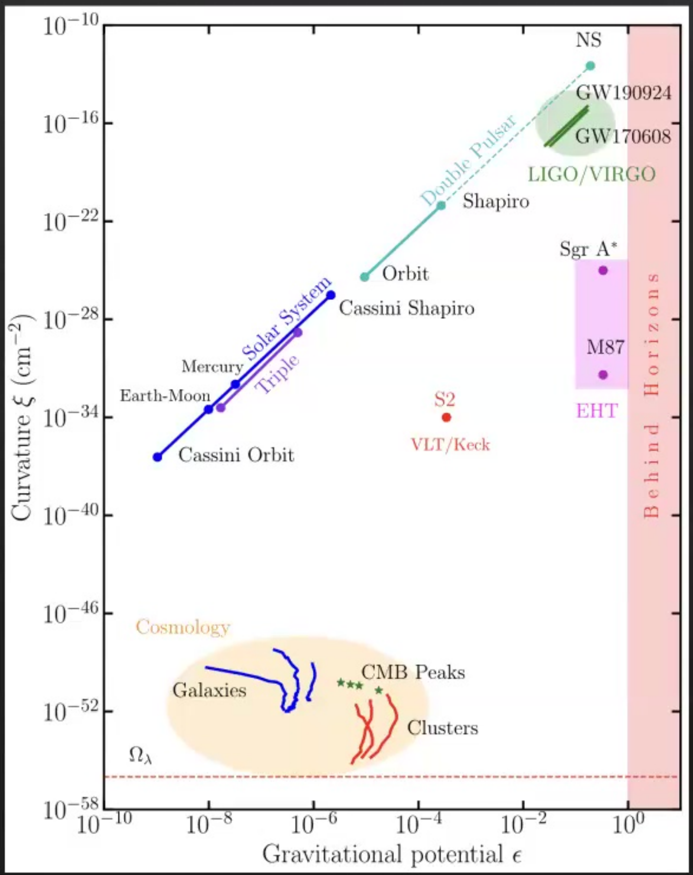

EHTC Sgr A* Paper VI, 2022

GWs from merger of stellar mass objects

Images of supermassive objects

GWs: Dynamical spacetimes, Radiative aspects of gravity

Images: Stationary spacetimes, motion of plasma

The Kerr Metric

The Kerr metric is a stationary, *vacuum* solution of GR

Can be read off from the line element:

$$ds^2 = g_{\alpha\beta}\mathrm{d}x^\alpha \mathrm{d}x^\beta = -\left(1 - \frac{2F}{\Sigma}\right)\mathrm{d}t^2 - 2\frac{2F}{\Sigma}a\sin^2\vartheta\,\mathrm{d}t\mathrm{d}\varphi + \frac{\Pi}{\Sigma}\sin^2\vartheta\,\mathrm{d}\varphi^2 + \frac{\Sigma}{\Delta}\mathrm{d}r^2 + \Sigma\,\mathrm{d}\vartheta^2$$

$$\begin{aligned} 2F(r) &= Mr \\ \Delta(r) &= r^2 - 2Mr + a^2 \\ \Sigma(r,\vartheta) &= r^2 + a^2\cos^2\vartheta \\ \Pi(r,\vartheta) &= (r^2+a^2)^2 - \Delta(r)a^2\sin^2\vartheta \end{aligned}$$

M is the mass
a is the specific angular momentum (a=J/M)

The Kerr Metric

The Kerr metric is a stationary, *vacuum* solution of GR

Can be read off from the line element:

$$\mathrm{d}s^2 = g_{\alpha\beta}\mathrm{d}x^\alpha \mathrm{d}x^\beta = -\left(1 - \frac{2F}{\Sigma}\right)\mathrm{d}t^2 - 2\frac{2F}{\Sigma}a\sin^2\vartheta\,\mathrm{d}t\mathrm{d}\varphi + \frac{\Pi}{\Sigma}\sin^2\vartheta\,\mathrm{d}\varphi^2 + \frac{\Sigma}{\Delta}\mathrm{d}r^2 + \Sigma\,\mathrm{d}\vartheta^2$$

$$\begin{aligned} 2F(r) &= Mr \\ \Delta(r) &= r^2 - 2Mr + a^2 \\ \Sigma(r,\vartheta) &= r^2 + a^2\cos^2\vartheta \\ \Pi(r,\vartheta) &= (r^2+a^2)^2 - \Delta(r)a^2\sin^2\vartheta \end{aligned}$$

Einstein equations

$$\mathcal{G}_{\mu\nu}(g_{\alpha\beta}) = \mathcal{T}_{\mu\nu}$$

Spacetime Einstein Tensor

Spacetime Metric Tensor

Matter Energy-Momentum-Stress Tensor

M is the mass
a is the specific angular momentum (a=J/M)

The Kerr metric describes black holes (BHs) when a <= M

The zero-spin (a=0) Kerr BH is the Schwarzschild BH

Kerr BHs are Structurally Simple

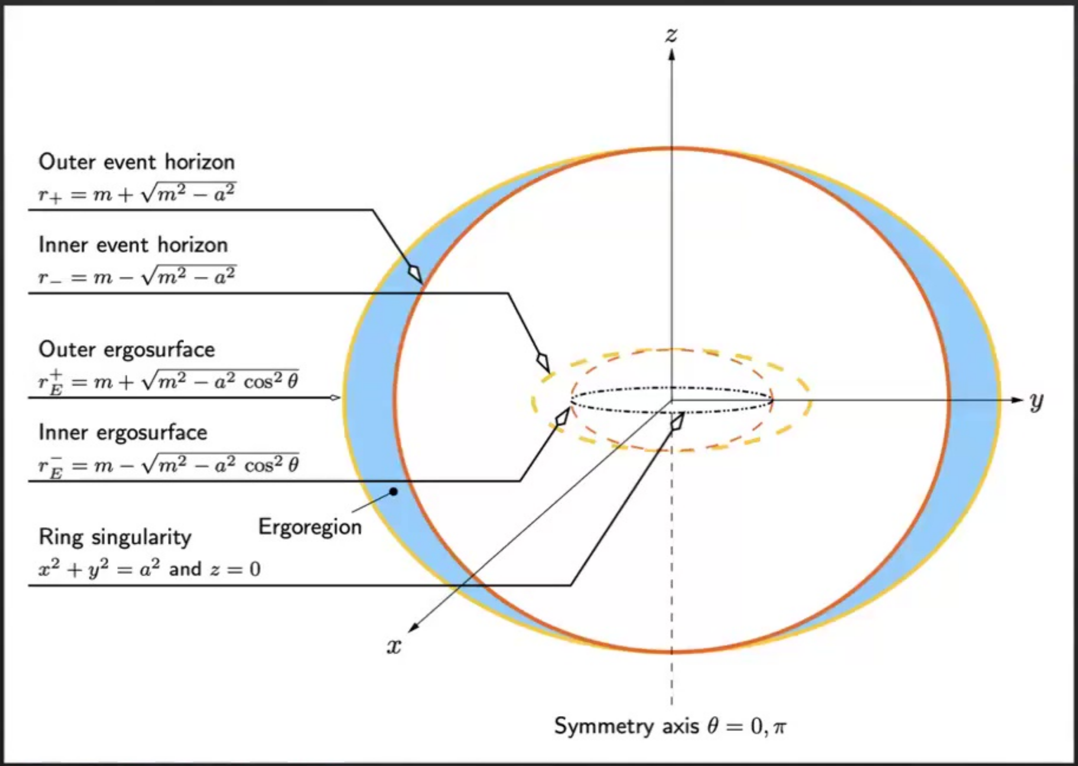

Visser, The Kerr Spacetime, 2008

By *tests of GR,* we actually mean *tests of the Kerr BH metric*

A very special metric indeed:
Everything determined by M and a: "*Kerr black holes have No other hair*"
(In particular, all higher-order multipoles of the metric are also set by M and a)

Some reasons to consider *Alternatives: Solution Metrics*

But they have problematic interiors:

[1] They contain a spacetime singularity
[2] The singularity can send signals to observers present inside the inner horizon
[3] Their inner horizon is unstable
[4] Interior is not stationary

Some reasons to consider *Alternatives: Solution Metrics*

Phenomenological Modifications:

~~*[1] They contain a spacetime singularity*~~

[2] The singularity can send signals to observers present inside the inner horizon

[3] Their inner horizon is unstable

$$\mathcal{G}_{\mu\nu}(g_{\alpha\beta}) = \mathcal{T}_{\mu\nu}$$

Some reasons to consider *Alternatives: Solution Metrics*

Phenomenological Modifications:

~~*[1] They contain a spacetime singularity*~~
~~*[2] The singularity can send signals to observers present inside the inner horizon*~~
~~*[3] Their inner horizon is unstable*~~

$$\mathscr{G}_{\mu\nu}(g_{\alpha\beta}) = \mathscr{T}_{\mu\nu}$$

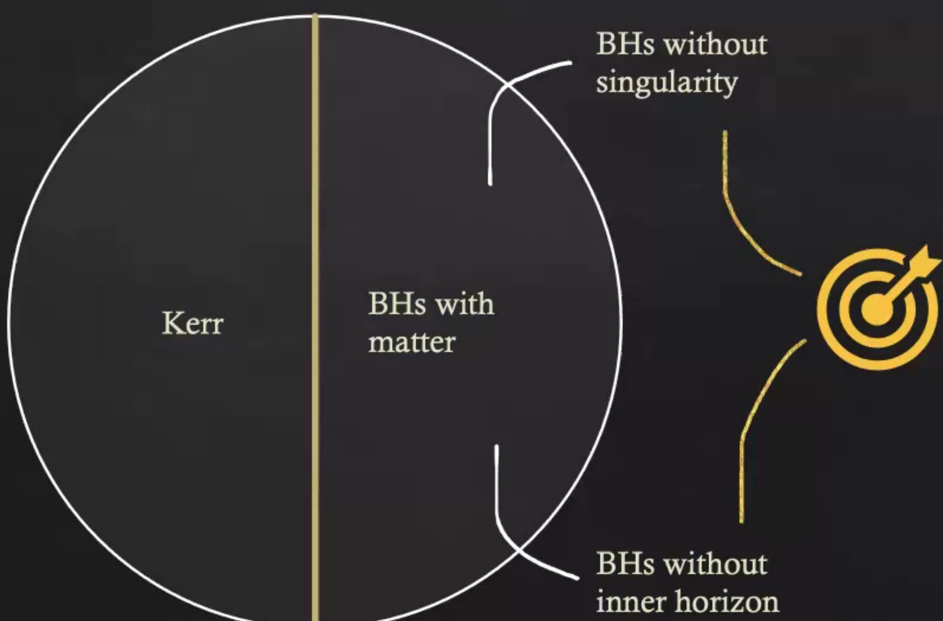

$$\mathscr{G}_{\mu\nu}(g_{\alpha\beta}) = \mathscr{T}_{\mu\nu}$$

Some reasons to consider *Alternatives:* Parametrized Metrics

Parametrized BH metrics are designed to perform agnostic tests of deviations from the Kerr metric

Konoplya-Rezzolla-Zhidenko

Rezzolla and Zhidenko, 2014
Konoplya, Rezzolla, Zhidenko, 2016
Kocherlakota and Rezzolla, 2020

Johannsen-Psaltis

Johannsen and Psaltis, 2011
Johannsen, 2013

. . .

Some reasons to consider *Alternatives:* Parametrized Metrics

Parametrized BH metrics are designed to perform agnostic tests of deviations from the Kerr metric

If you interpret them as solutions to GR, they must have some nonzero matter content

$$\mathcal{G}_{\mu\nu}(g_{\alpha\beta}) = \mathcal{T}_{\mu\nu}$$

Konoplya-Rezzolla-Zhidenko

Rezzolla and Zhidenko, 2014
Konoplya, Rezzolla, Zhidenko, 2016
Kocherlakota and Rezzolla, 2020

Johannsen-Psaltis

Johannsen and Psaltis, 2011
Johannsen, 2013

...

General Spherically-Symmetric Black Holes

Metric: $$\mathrm{d}s^2 = -f(r)\mathrm{d}t^2 + \frac{g(r)}{f(r)}\mathrm{d}r^2 + R^2(r)\mathrm{d}\Omega_2^2$$

Schwarzschild:

$$f(r) = 1 - \frac{2M}{r}\,;\quad g(r) = 1\,;\quad R(r) = r$$

Solving for photon orbits is extremely simple since they have four conserved quantities:
Rest-Mass; Energy; **Azimuthal Angular Momentum**; **Total Angular Momentum**

Reminiscent of the Kepler problem.
Indeed, all particles (incl. photons) move on planar orbits

General Spherically-Symmetric Black Holes

Metric: $$ds^2 = -f(r)dt^2 + \frac{g(r)}{f(r)}dr^2 + R^2(r)d\Omega_2^2$$

Schwarzschild: $$f(r) = 1 - \frac{2M}{r}\,; \quad g(r) = 1\,; \quad R(r) = r$$

Solving for photon orbits is extremely simple since they have four conserved quantities:
Rest-Mass; **Energy**; Azimuthal Angular Momentum; **Total Angular Momentum**

The impact parameter of the photon is simply the ratio of these quantities $$\eta = \frac{L}{E}$$

Photons can move on circular orbits, at the *photon sphere*.
The radius and impact parameter of such a photon:

$$\frac{\partial_r f}{f} - 2\frac{\partial_r R}{R} = 0\,; \quad \eta_{\mathrm{PS}} = \frac{R_{\mathrm{PS}}}{\sqrt{f_{\mathrm{PS}}}}$$

Notation: $R_{\mathrm{PS}} = R(r_{\mathrm{PS}})$

General Spherically-Symmetric Black Holes

Metric: $$ds^2 = -f(r)dt^2 + \frac{g(r)}{f(r)}dr^2 + R^2(r)d\Omega_2^2$$

Schwarzschild: $f(r) = 1 - \frac{2M}{r}$; $g(r) = 1$; $R(r) = r$

Solving for photon orbits is extremely simple since they have four conserved quantities:
Rest-Mass; **Energy**; Azimuthal Angular Momentum; **Total Angular Momentum**

The impact parameter of the photon is simply the ratio of these quantities $$\eta = \frac{L}{E}$$

Photons can move on circular orbits, at the *photon sphere*.
The radius and impact parameter of such a photon:

$$\frac{\partial_r f}{f} - 2\frac{\partial_r R}{R} = 0 \, ; \quad \eta_{PS} = \frac{R_{PS}}{\sqrt{f_{PS}}}$$

Notation: $R_{PS} = R(r_{PS})$

Connection between the Emission Ring & the Shadow Boundary

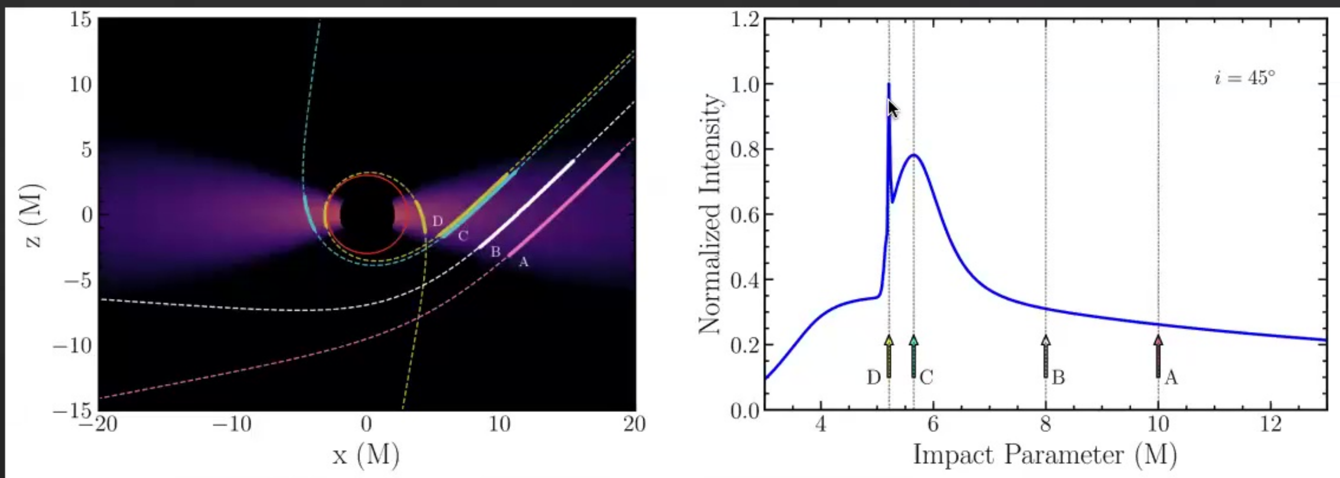

Ozel, Psaltis, Younsi, 2023

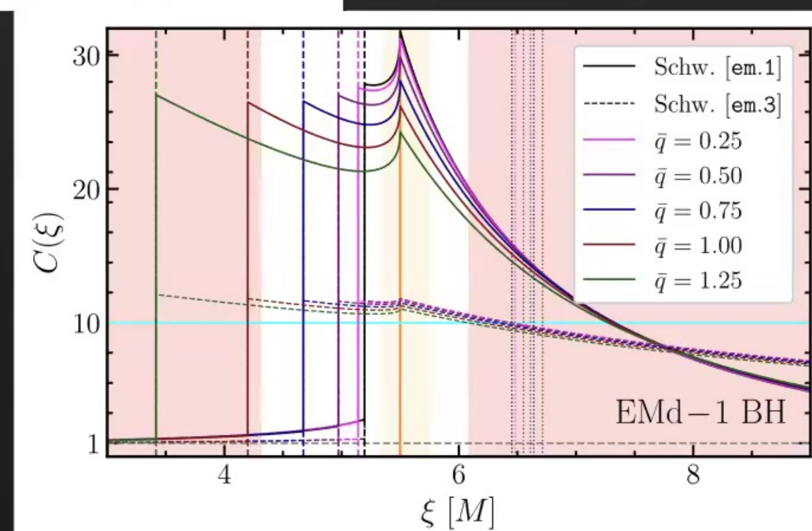

Kocherlakota & Rezzolla, 2022

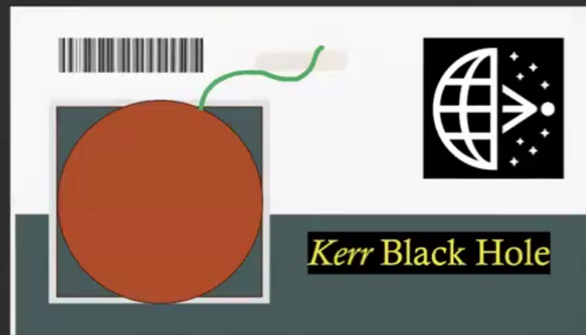

First M87 Event Horizon Telescope Results. VI. The Shadow and Mass of the Central Black Hole

The Event Horizon Telescope Collaboration
(See the end matter for the full list of authors.)
Received 2019 March 8; revised 2019 March 18; accepted 2019 March 20; published 2019 April 10

Abstract

We present measurements of the properties of the central radio source in M87 using Event Horizon Telescope data obtained during the 2017 campaign. We develop and fit geometric crescent models (asymmetric rings with interior brightness depressions) using two independent sampling algorithms that consider distinct representations of the visibility data. We show that the crescent family of models is statistically preferred over other comparably complex geometric models that we explore. We calibrate the geometric model parameters using general relativistic magnetohydrodynamic (GRMHD) models of the emission region and estimate physical properties of the source. We further fit images generated from GRMHD models directly to the data. We compare the derived emission region and black hole parameters from these analyses with those recovered from reconstructed images. There is a remarkable consistency among all methods and data sets. We find that >50% of the total flux at arcsecond scales comes from near the horizon, and that the emission is dramatically suppressed interior to this region by a factor >10, providing direct evidence of the predicted shadow of a black hole. Across all methods, we measure a crescent diameter of $42 \pm 3\,\mu$as and constrain its fractional width to be <0.5. Associating the crescent feature with the emission surrounding the black hole shadow, we infer an angular gravitational radius of $GM/Dc^2 = 3.8 \pm 0.4\,\mu$as. Folding in a distance measurement of $16.8^{+0.8}_{-0.7}$ Mpc gives a black hole mass of $M = 6.5 \pm 0.2|_{\rm stat} \pm 0.7|_{\rm sys} \times 10^9\,M_\odot$. This measurement from lensed emission near the event horizon is consistent with the presence of a central Kerr black hole, as predicted by the general theory of relativity.

Higher-Order
Post-Newtonian Parameters

Gravitational Test beyond the First Post-Newtonian Order with the Shadow of the M87 Black Hole

Dimitrios Psaltis,[1] Lia Medeiros,[2] Pierre Christian,[1] Feryal Özel,[1] Kazunori Akiyama,[3–6] Antxon Alberdi,[7] Walter Alef,[8]
(EHT Collaboration)

(Received 26 May 2020; accepted 31 August 2020; published 1 October 2020)

The 2017 Event Horizon Telescope (EHT) observations of the central source in M87 have led to the first measurement of the size of a black-hole shadow. This observation offers a new and clean gravitational test of the black-hole metric in the strong-field regime. We show analytically that spacetimes that deviate from the Kerr metric but satisfy weak-field tests can lead to large deviations in the predicted black-hole shadows that are inconsistent with even the current EHT measurements. We use numerical calculations of regular, parametric, non-Kerr metrics to identify the common characteristic among these different parametrizations that control the predicted shadow size. We show that the shadow-size measurements place significant constraints on deviation parameters that control the second post-Newtonian and higher orders of each metric and are, therefore, inaccessible to weak-field tests. The new constraints are complementary to those imposed by observations of gravitational waves from stellar-mass sources.

Alternative

- *GR black hole models*
- *theories of gravity*
- *non-BH models*

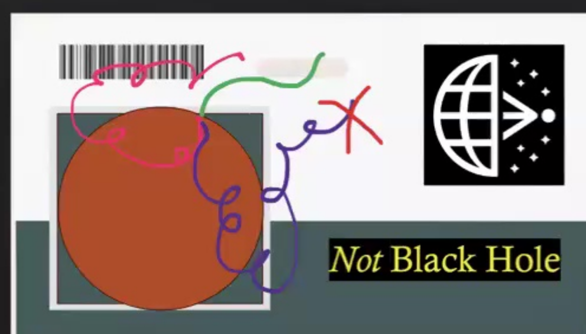

Constraints on black-hole charges with the 2017 EHT observations of M87*

Prashant Kocherlakota,[1] Luciano Rezzolla,[1–3] Heino Falcke,[4] Christian M. Fromm,[5,6,1] Michael Kramer,[7] Yosuke Mizuno,[8,9] Antonios Nathanail,[9,10] Héctor Olivares,[4] Ziri Younsi,[11,9] Kazunori Akiyama,[12,13,5] Antxon Alberdi,[14]
(EHT Collaboration)

(Received 29 November 2020; accepted 21 April 2021; published 20 May 2021)

Our understanding of strong gravity near supermassive compact objects has recently improved thanks to the measurements made by the Event Horizon Telescope (EHT). We use here the M87* shadow size to infer constraints on the physical charges of a large variety of nonrotating or rotating black holes. For example, we show that the quality of the measurements is already sufficient to rule out that M87* is a highly charged dilaton black hole. Similarly, when considering black holes with two physical and independent charges, we are able to exclude considerable regions of the space of parameters for the doubly-charged dilaton and the Sen black holes.

Higher-Order
Post-Newtonian Parameters

Alternative

- *GR black hole models*
- *theories of gravity*
- *non-BH models*

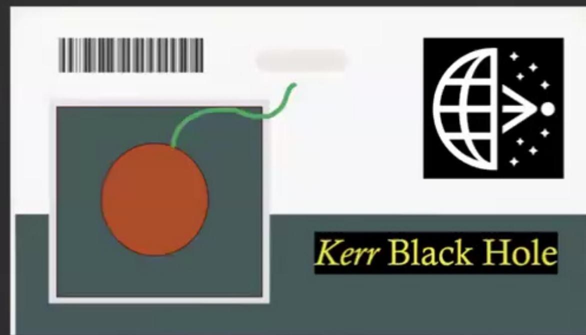

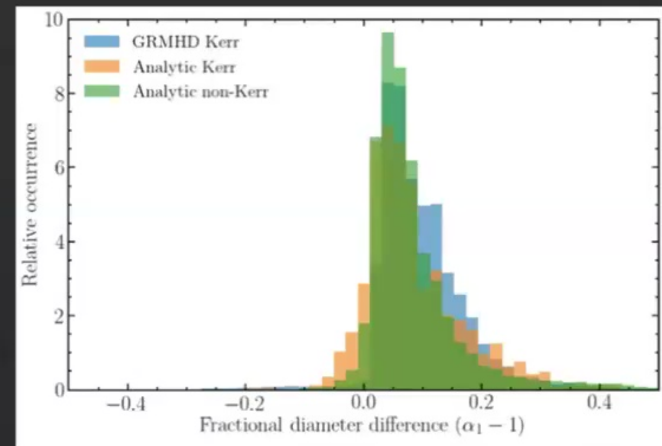

Quantifying offset

First Sagittarius A* Event Horizon Telescope Results. VI. Testing the Black Hole Metric

The Event Horizon Telescope Collaboration
(See the end matter for the full list of authors.)

Received 2022 March 15; revised 2022 April 12; accepted 2022 April 12; published 2022 May 12

Abstract

Astrophysical black holes are expected to be described by the Kerr metric. This is the only stationary, vacuum, axisymmetric metric, without electromagnetic charge, that satisfies Einstein's equations and does not have pathologies outside of the event horizon. We present new constraints on potential deviations from the Kerr prediction based on 2017 EHT observations of Sagittarius A* (Sgr A*). We calibrate the relationship between the geometrically defined black hole shadow and the observed size of the ring-like images using a library that includes both Kerr and non-Kerr simulations. We use the exquisite prior constraints on the mass-to-distance ratio for Sgr A* to show that the observed image size is within ∼10% of the Kerr predictions. We use these bounds to constrain metrics that are parametrically different from Kerr, as well as the charges of several known spacetimes. To consider alternatives to the presence of an event horizon, we explore the possibility that Sgr A* is a compact object with a surface that either absorbs and thermally reemits incident radiation or partially reflects it. Using the observed image size and the broadband spectrum of Sgr A*, we conclude that a thermal surface can be ruled out and a fully reflective one is unlikely. We compare our results to the broader landscape of gravitational tests. Together with the bounds found for stellar-mass black holes and the M87 black hole, our observations provide further support that the external spacetimes of all black holes are described by the Kerr metric, independent of their mass.

Surfaces

- *thermalizing*
- *reflecting*

Future Black Hole Imaging: *The Photon Ring*

[Credit: Abhishek Joshi]

A sample movie of a simulation of hot accretion onto a Kerr black hole

[Credit: Vedant Dhruv]

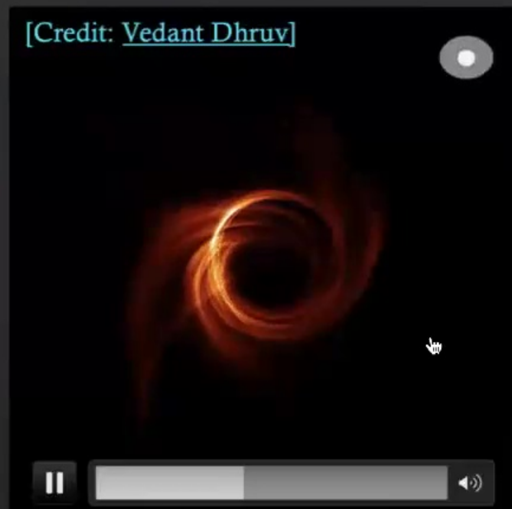

Effect of viewing angle

George Wong and Michael Johnson

Johnson et al., 2020

Composition of higher-order images of the entire accretion flow

Higher-Order Images

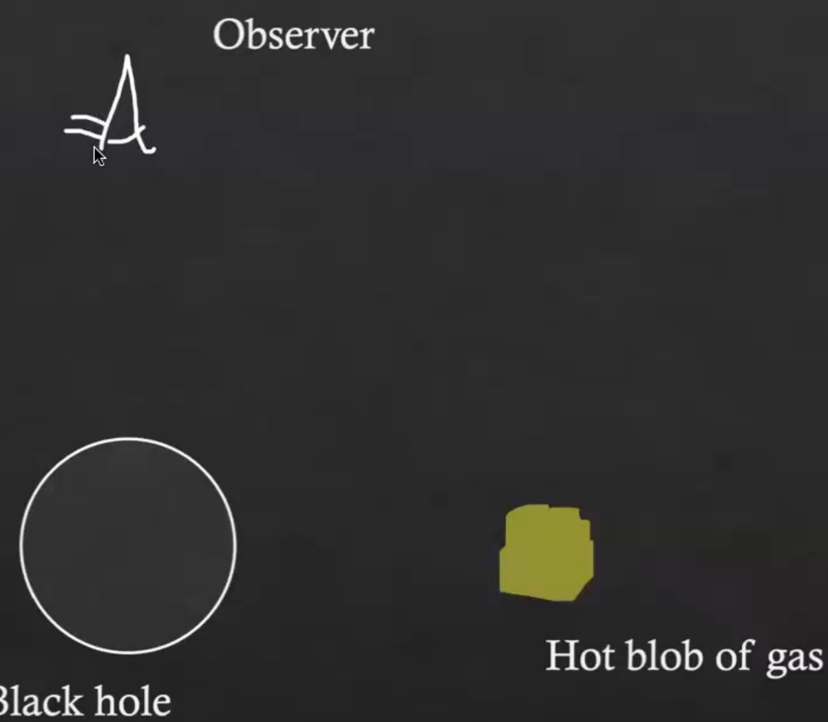

Bardeen, Press, Teukolsky, 1972
Luminet, 1979
…
Gralla, Holz, Wald, 2019
Johnson et al., 2020
…

Higher-Order Images

$$
\begin{aligned}
\Delta\vartheta &= (\vartheta_{\mathrm{obs}} - \vartheta_{\mathrm{emit}}) \mod 2\pi \\
&= -\vartheta_{\mathrm{emit}} \mod 2\pi \\
&= -\vartheta_{\mathrm{emit}} \pm 2\pi m
\end{aligned}
$$

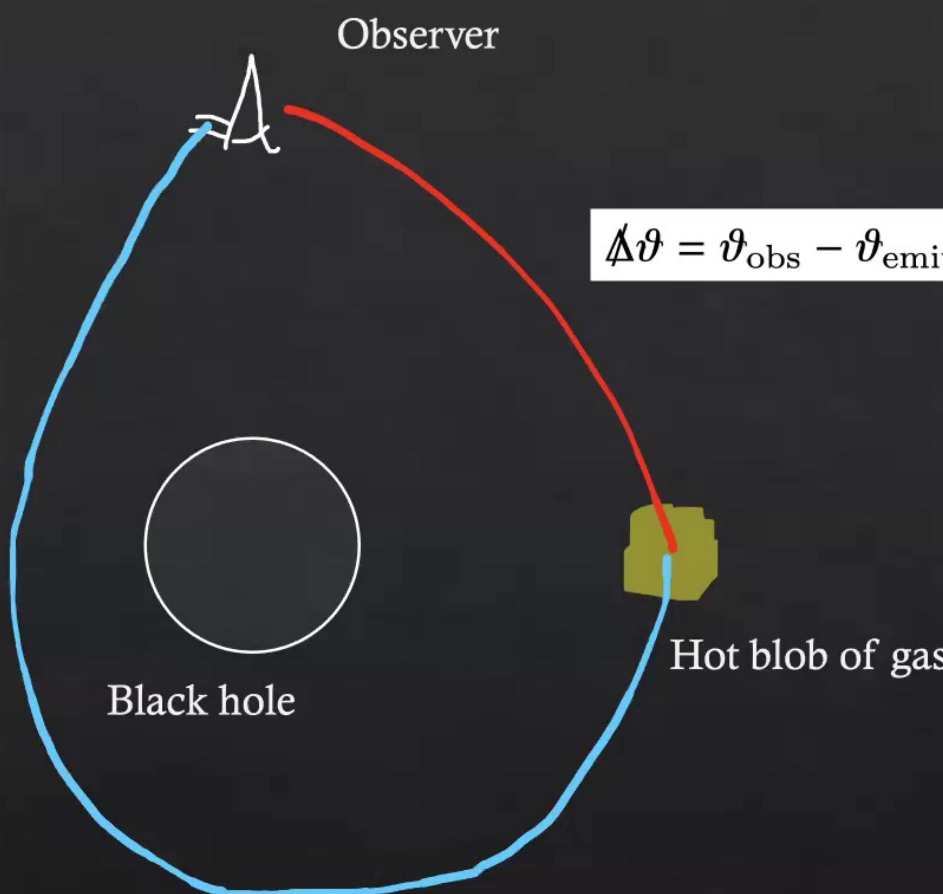

$$\Delta\vartheta = \vartheta_{\mathrm{obs}} - \vartheta_{\mathrm{emit}} = -\vartheta_{\mathrm{emit}}$$

Bardeen, Press, Teukolsky, 1972
Luminet, 1979
…
Gralla, Holz, Wald, 2019
Johnson et al., 2020
…

Higher-Order Images

$$\Delta\vartheta = (\vartheta_{\text{obs}} - \vartheta_{\text{emit}}) \mod 2\pi$$
$$= -\vartheta_{\text{emit}} \mod 2\pi$$
$$= -\vartheta_{\text{emit}} \pm 2\pi m$$

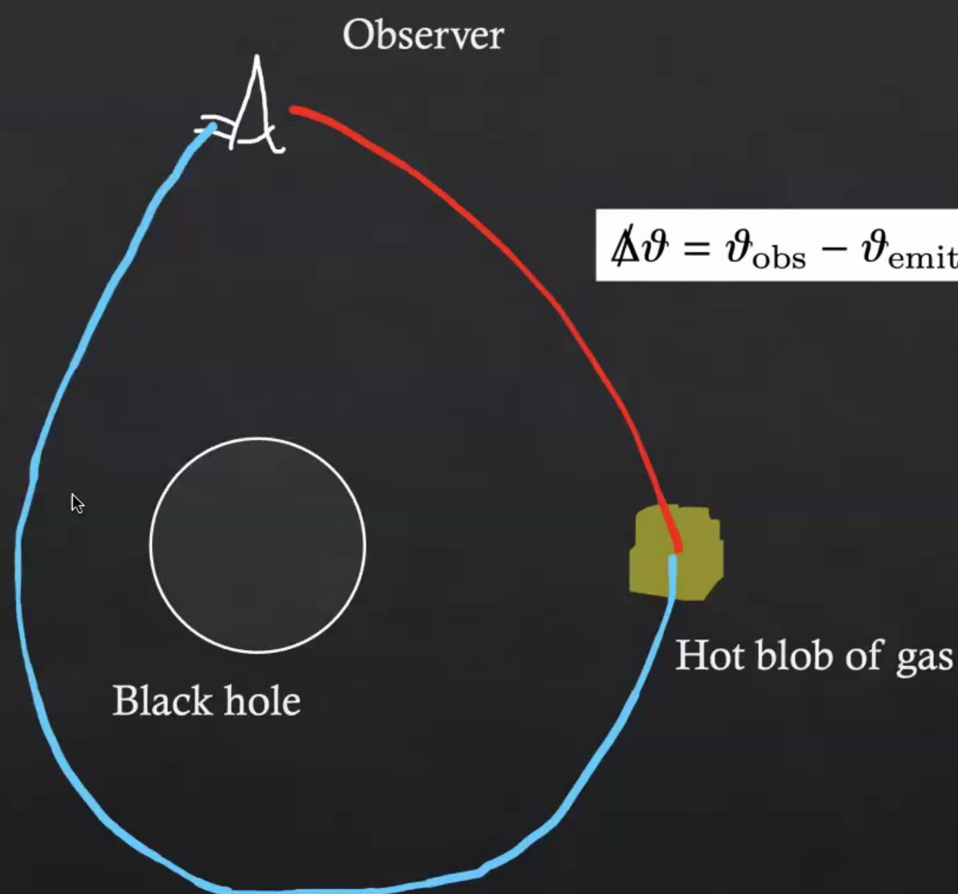

$$\Delta\vartheta = \vartheta_{\text{obs}} - \vartheta_{\text{emit}} = -\vartheta_{\text{emit}}$$

Increasing deflection in the following order:
(-, 0); (+, 1); (-, 1); (+,2) …

Replace this by n, i.e.,

(-, 0) → n=0
(+, 1) → n=1
(-, 1) → n=2

Bardeen, Press, Teukolsky, 1972
Luminet, 1979
…
Gralla, Holz, Wald, 2019
Johnson et al., 2020
…

Higher-Order Images: Schwarzschild BH

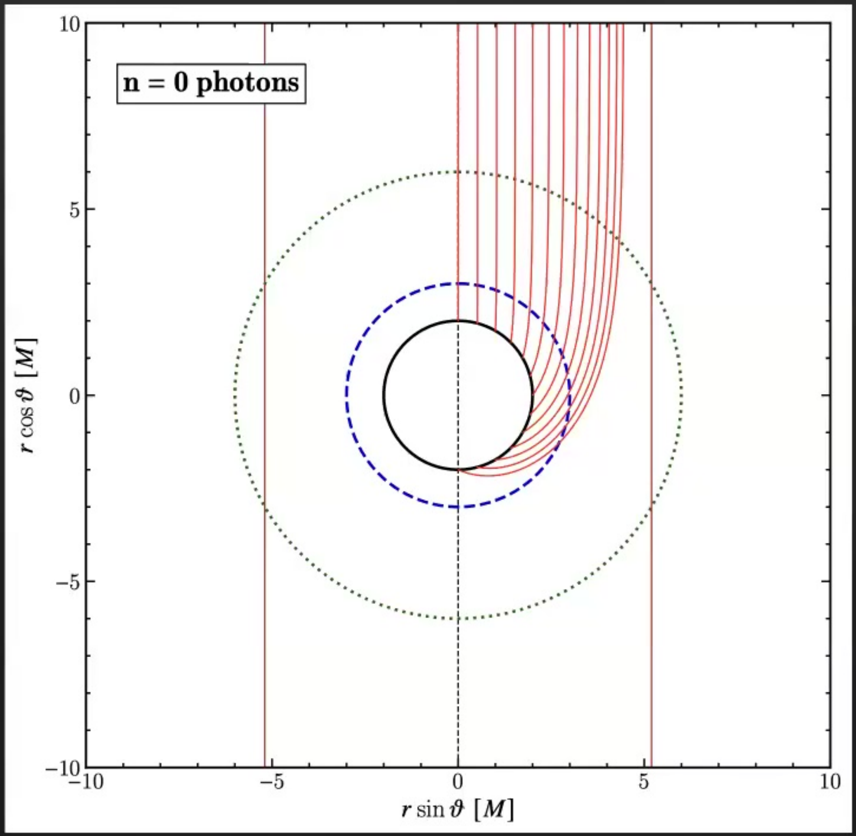

Higher-Order Images: Schwarzschild BH

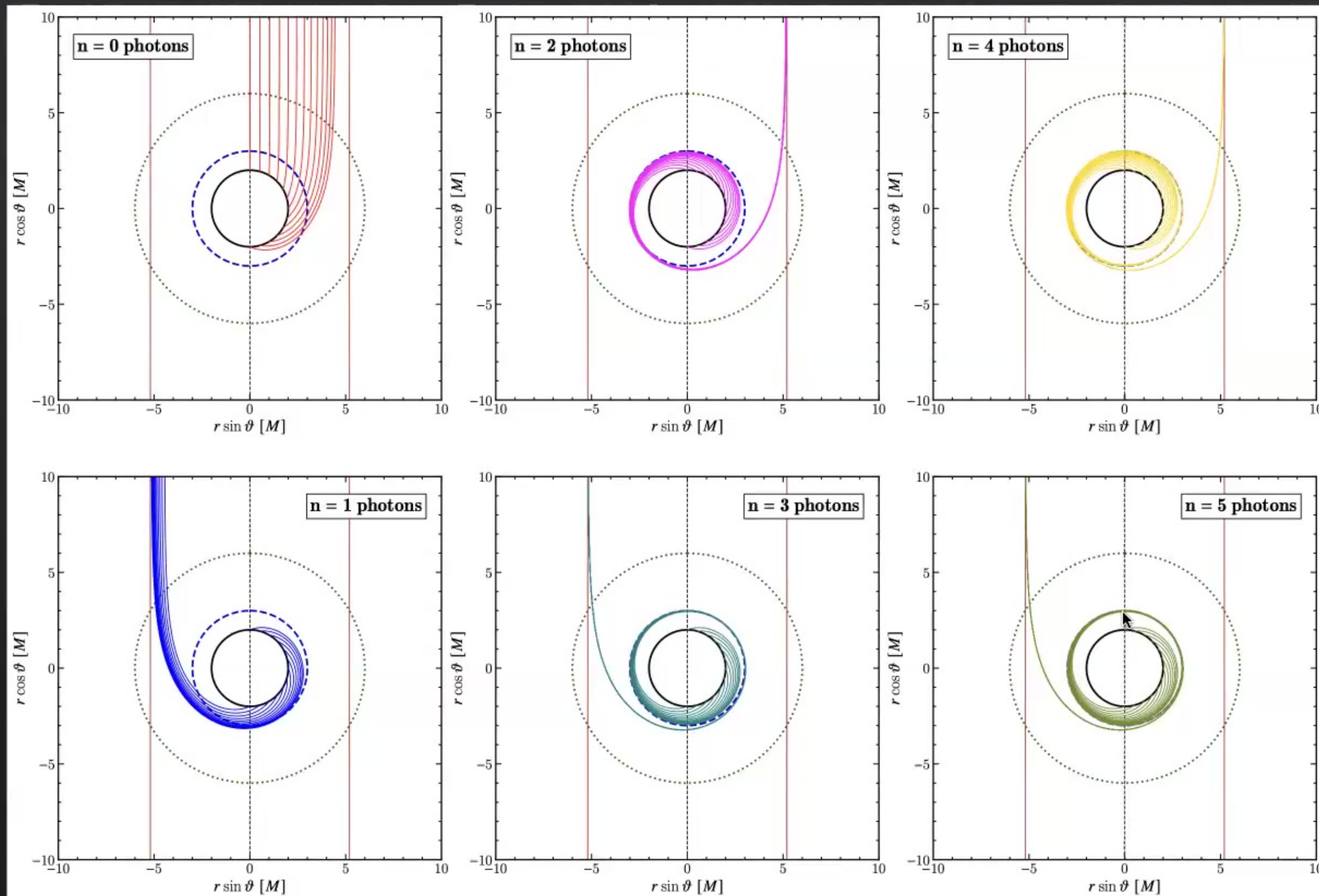

Higher-Order Images: Schwarzschild BH

Region on the image plane collecting all higher-order images: Photon Ring

$$\frac{\eta_{n+1} - \eta_{\rm PS}}{\eta_n - \eta_{\rm PS}} \approx e^{-\gamma_{\rm PS}}$$

Bardeen, Press, Teukolsky, 1972
Luminet, 1979
…
Gralla, Holz, Wald, 2019
Johnson et al., 2020

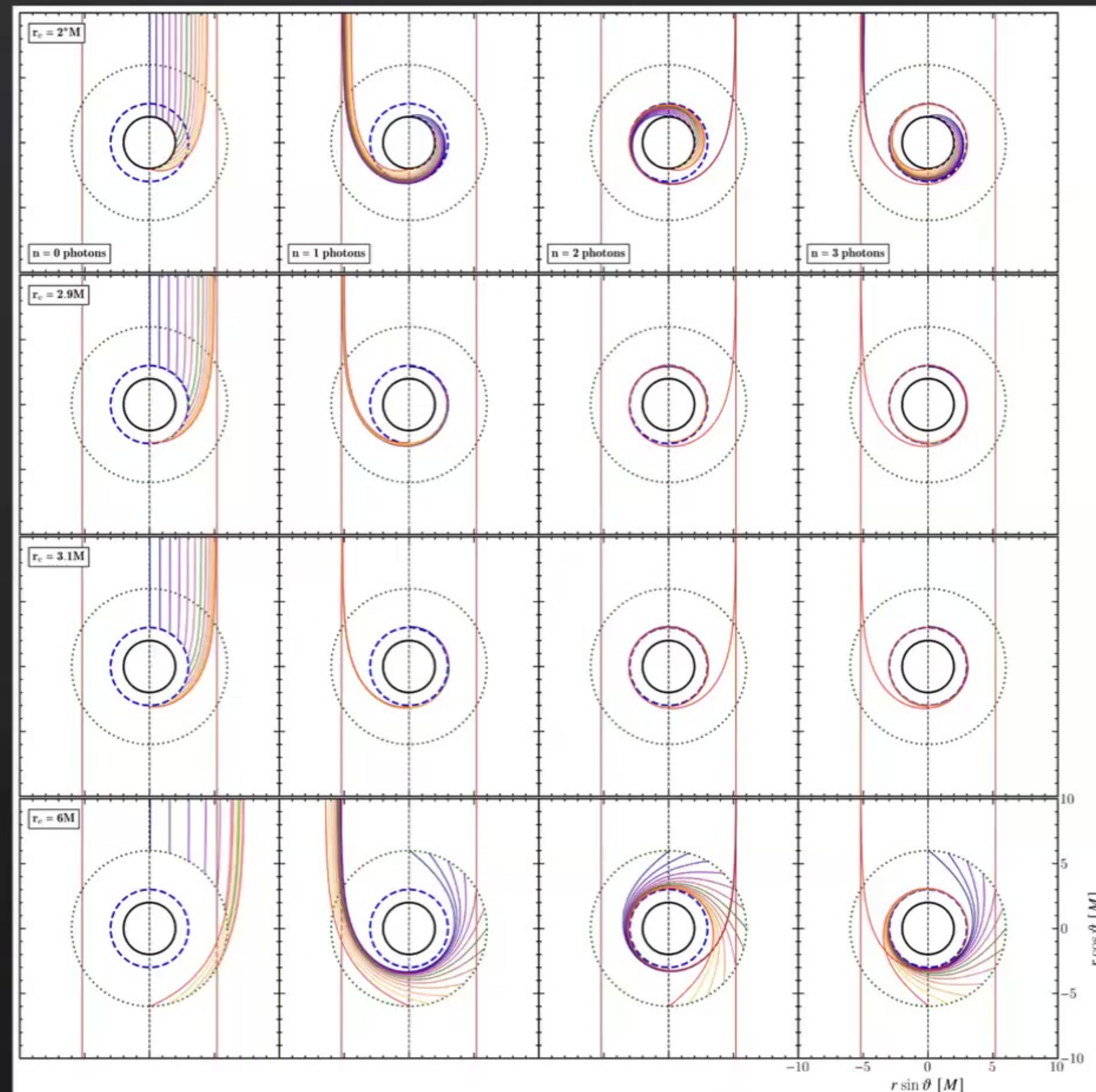

Kocherlakota et al., 2024a

The Photon Ring & Universal Relations

Due to *extreme*-lensing at the photon shell

$$\not{\Delta}\vartheta \approx -\frac{\pi}{\gamma_{\rm PS}} \ln|\bar{\eta}|$$

To link the image radii of different order images, notice that (equatorial source)

$$\not{\Delta}\vartheta_{n+1} - \not{\Delta}\vartheta_n = \pi$$

$$\frac{\eta_{n+1} - \eta_{\rm PS}}{\eta_n - \eta_{\rm PS}} \approx e^{-\gamma_{\rm PS}}$$

Lensing Lyapunov Exponent

The time delay between the appearance of these images is

$$\not{\Delta}t_{n+1} - \not{\Delta}t_n \approx t_{\rm d;PS} = \pi\eta_{\rm PS} = \frac{\pi}{\Omega_{\rm PS}}$$

Orbital angular velocity of circular photon orbit

Shadow size!

also:
Bozza and Scarpetta, 2007
Gralla, Holz, Wald, 2019
Johnson et al., 2020
Gralla and Lupsasca, 2020
Broderick, Salehi, Georgiev 2023
Salehi, Broderick, Georgiev 2024

Kocherlakota et al., 2024a

The Spacetime Critical Parameters

Metric

$$\mathrm{d}s^2 = -f(r)\mathrm{d}t^2 + \frac{g(r)}{f(r)}\mathrm{d}r^2 + R^2(r)\mathrm{d}\Omega_2^2$$

Photon Sphere & Shadow Radius

$$\frac{\partial_r f}{f} - 2\frac{\partial_r R}{R} = 0\,; \quad \eta_{\mathrm{PS}} = \frac{R_{\mathrm{PS}}}{\sqrt{f_{\mathrm{PS}}}}$$

Lensing Lyapunov Exponent

$$\gamma_{\mathrm{PS}} := \frac{\pi R_{\mathrm{PS}}^2}{\eta_{\mathrm{PS}}}\hat{\kappa}_{\mathrm{PS}}$$

Phase-Space Lyapunov Exponent

$$\hat{\kappa}_{\mathrm{PS}}^2 := \frac{1}{2g_{\mathrm{PS}}}\left(\frac{\partial_r^2 R_{\mathrm{PS}}^2}{R_{\mathrm{PS}}^2} - \frac{\partial_r^2 f_{\mathrm{PS}}}{f_{\mathrm{PS}}}\right)$$

Kocherlakota et al., 2024a

The Spacetime Critical Parameters

Metric	$\mathrm{d}s^2 = -f(r)\mathrm{d}t^2 + \frac{g(r)}{f(r)}\mathrm{d}r^2 + R^2(r)\mathrm{d}\Omega_2^2$
Photon Sphere & Shadow Radius	$\frac{\partial_r f}{f} - 2\frac{\partial_r R}{R} = 0\,; \quad \eta_{\mathrm{PS}} = \frac{R_{\mathrm{PS}}}{\sqrt{f_{\mathrm{PS}}}}$
Lensing Lyapunov Exponent	$\gamma_{\mathrm{PS}} := \frac{\pi R_{\mathrm{PS}}^2}{\eta_{\mathrm{PS}}}\hat{\kappa}_{\mathrm{PS}}$
Phase-Space Lyapunov Exponent	$\hat{\kappa}_{\mathrm{PS}}^2 := \frac{1}{2g_{\mathrm{PS}}}\left(\frac{\partial_r^2 R_{\mathrm{PS}}^2}{R_{\mathrm{PS}}^2} - \frac{\partial_r^2 f_{\mathrm{PS}}}{f_{\mathrm{PS}}}\right)$
Lyapunov Time	$t_{\ell;\mathrm{PS}} := \frac{1}{f_{\mathrm{PS}}\hat{\kappa}_{\mathrm{PS}}}$

$$\frac{r(t) - r_{\mathrm{PS}}}{r(0) - r_{\mathrm{PS}}} \approx \mathrm{e}^{-t/t_{\ell;\mathrm{PS}}}$$

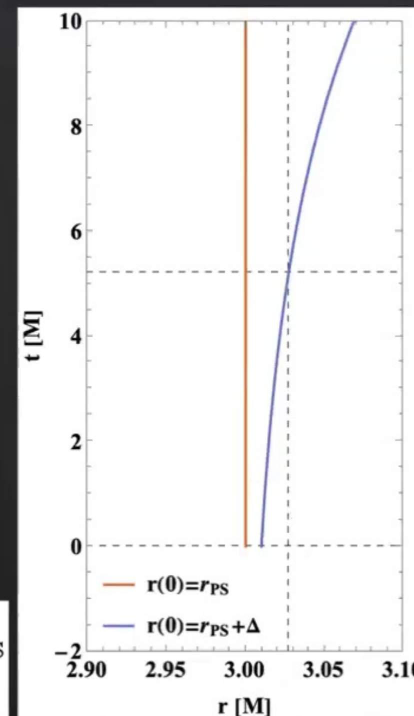

Kocherlakota et al., 2024a

The Spacetime Critical Parameters

Metric

$$\mathrm{d}s^2 = -f(r)\mathrm{d}t^2 + \frac{g(r)}{f(r)}\mathrm{d}r^2 + R^2(r)\mathrm{d}\Omega_2^2$$

Photon Sphere & Shadow Radius

$$\frac{\partial_r f}{f} - 2\frac{\partial_r R}{R} = 0\,; \quad \eta_{\mathrm{PS}} = \frac{R_{\mathrm{PS}}}{\sqrt{f_{\mathrm{PS}}}}$$

Lensing Lyapunov Exponent

$$\gamma_{\mathrm{PS}} := \frac{\pi R_{\mathrm{PS}}^2}{\eta_{\mathrm{PS}}}\hat{\kappa}_{\mathrm{PS}}$$

Phase-Space Lyapunov Exponent

$$\hat{\kappa}_{\mathrm{PS}}^2 := \frac{1}{2g_{\mathrm{PS}}}\left(\frac{\partial_r^2 R_{\mathrm{PS}}^2}{R_{\mathrm{PS}}^2} - \frac{\partial_r^2 f_{\mathrm{PS}}}{f_{\mathrm{PS}}}\right)$$

Lyapunov Time

$$t_{\ell;\mathrm{PS}} := \frac{1}{f_{\mathrm{PS}}\hat{\kappa}_{\mathrm{PS}}}$$

Alternative Path to obtain Lensing Lyapunov Exponent

$$\frac{t_{\mathrm{d};\mathrm{PS}}}{t_{\ell;\mathrm{PS}}} = \gamma_{\mathrm{PS}}$$

Kocherlakota et al., 2024a

The Spacetime Critical Parameters

		Schwarzschild
Metric	$\mathrm{d}s^2 = -f(r)\mathrm{d}t^2 + \frac{g(r)}{f(r)}\mathrm{d}r^2 + R^2(r)\mathrm{d}\Omega_2^2$	$f(r) = 1 - \frac{2M}{r}\,;\ \ g(r) = 1\,;\ \ R(r) = r$
Photon Sphere & Shadow Radius	$\frac{\partial_r f}{f} - 2\frac{\partial_r R}{R} = 0\,;\quad \eta_{\mathrm{PS}} = \frac{R_{\mathrm{PS}}}{\sqrt{f_{\mathrm{PS}}}}$	$r_{\mathrm{PS}} = 3M\,;\ \ \eta_{\mathrm{PS}} = \sqrt{27}M$
Lensing Lyapunov Exponent	$\gamma_{\mathrm{PS}} := \frac{\pi R_{\mathrm{PS}}^2}{\eta_{\mathrm{PS}}}\hat{\kappa}_{\mathrm{PS}}$	$\gamma_{\mathrm{PS}} = \pi$
Phase-Space Lyapunov Exponent	$\hat{\kappa}_{\mathrm{PS}}^2 := \frac{1}{2g_{\mathrm{PS}}}\left(\frac{\partial_r^2 R_{\mathrm{PS}}^2}{R_{\mathrm{PS}}^2} - \frac{\partial_r^2 f_{\mathrm{PS}}}{f_{\mathrm{PS}}}\right)$	$\hat{\kappa}_{\mathrm{PS}} = 1/(\sqrt{3}M)$
Lyapunov Time	$t_{\ell;\mathrm{PS}} := \frac{1}{f_{\mathrm{PS}}\hat{\kappa}_{\mathrm{PS}}}$	$t_{\ell;\mathrm{PS}} = \sqrt{27}M$

Cardoso, Miranda, Berti, Witek, and Zanchin, 2009

Alternative Path to obtain Lensing Lyapunov Exponent

$$\frac{t_{\mathrm{d;PS}}}{t_{\ell;\mathrm{PS}}} = \gamma_{\mathrm{PS}}$$

Synergy with GWs

$$\omega_{\mathrm{QNM}} = l\left(\frac{1}{\eta_{\mathrm{PS}}}\right) - \mathrm{i}\left(n + \frac{1}{2}\right)\left(\frac{1}{t_{\ell;\mathrm{PS}}}\right)$$

Higher-Order Images of Hotspots:
The Delay Time

Flaring events associated with Sgr A* modeled as a hotspot

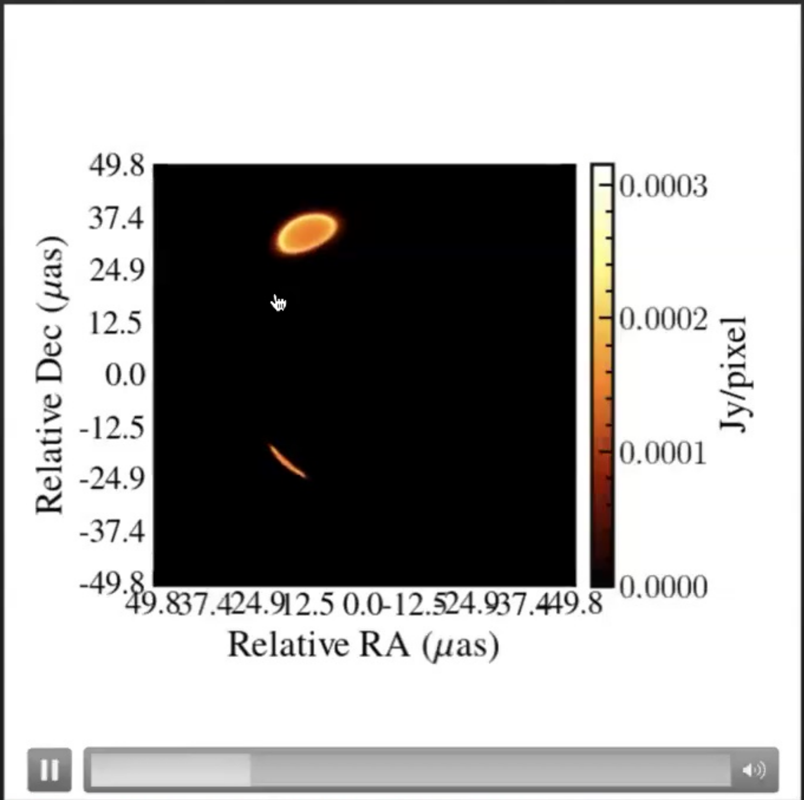

D. Jones, P. Kocherlakota, P. Tiede, D. Chang, K. Chatterjee

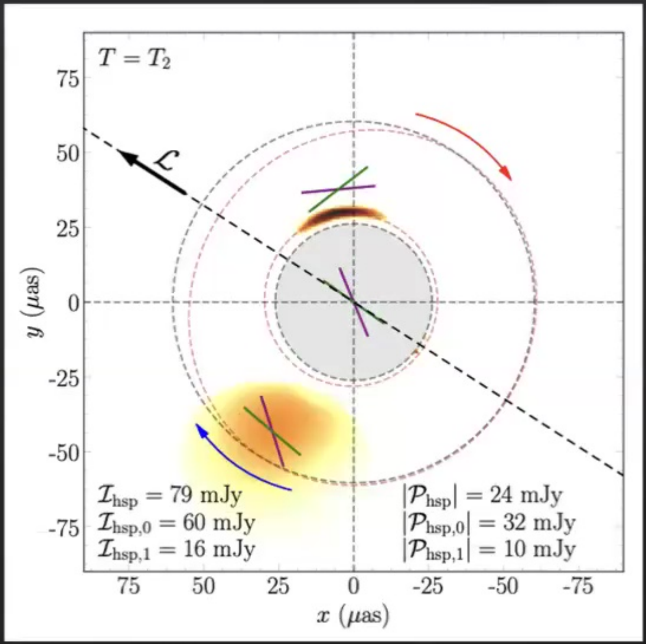

Wielgus et al., 2022

Wong, 2021
Ball et al., 2021
Wielgus et al., 2022
Vos et al., 2022
Emami et al., 2023
Vos et al., 2023
Yfantis et al., 2023

From the Delay Time to the Shadow Size

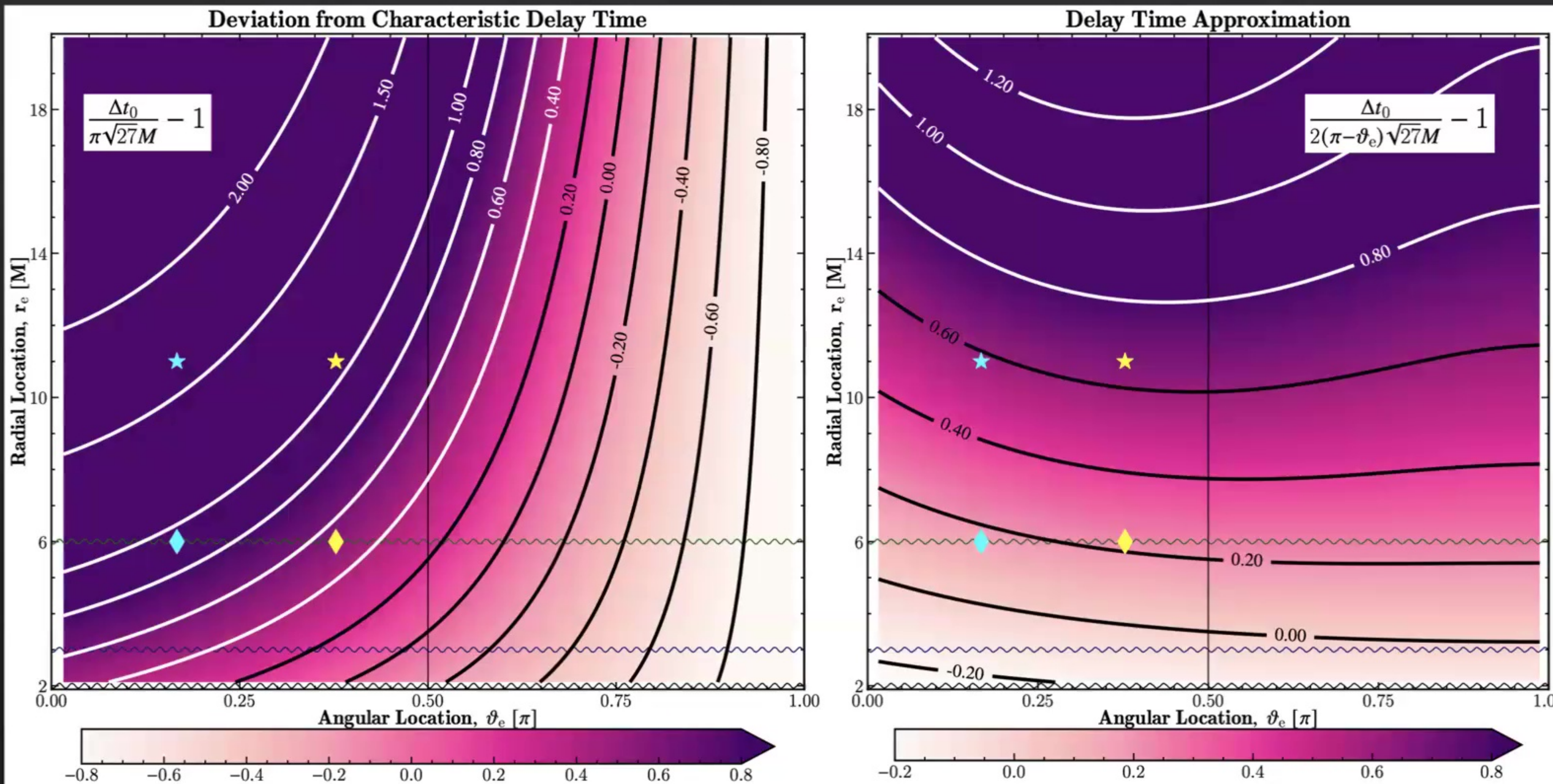

Kocherlakota, Rezzolla, Roy, Wielgus 2024b

Higher-Order Images of Accretion Flows: *The Lensing Lyapunov Exponent*

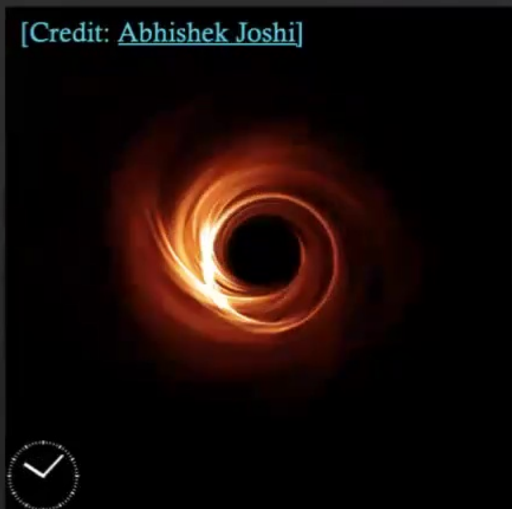

A sample movie of a simulation of hot accretion onto a Kerr black hole

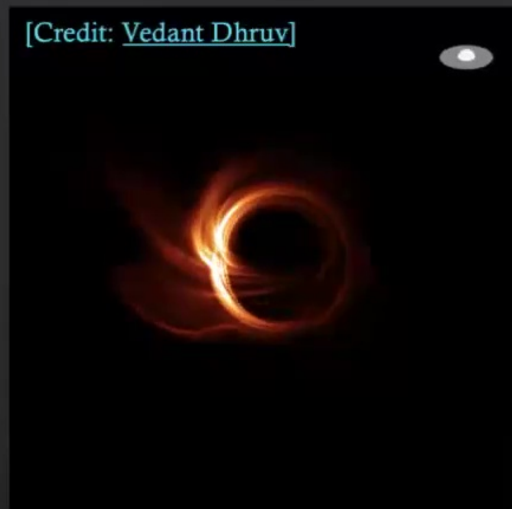

Effect of viewing angle

George Wong and Michael Johnson

Johnson et al., 2020

Higher-Order Images of Accretion Flows: *The Lensing Lyapunov Exponent*

[Credit: Abhishek Joshi]

A sample movie of a simulation of hot accretion onto a Kerr black hole

[Credit: Vedant Dhruv]

Effect of viewing angle

George Wong and Michael Johnson

Johnson et al., 2020

We saw for point sources:

$$\frac{\eta_{n+1} - \eta_{\mathrm{PS}}}{\eta_n - \eta_{\mathrm{PS}}} \approx \mathrm{e}^{-\gamma_{\mathrm{PS}}}$$

Johnson et al., 2020

Now for extended sources:

$$\frac{d_{n+1} - d_{\mathrm{sh}}}{d_n - d_{\mathrm{sh}}} \approx \frac{w_{n+1}}{w_n} \approx \frac{F_{n+1}}{F_n} \approx \mathrm{e}^{-\gamma_{\mathrm{PS}}}$$

Kocherlakota et al., 2024a

Late Time Luminosity Behavior of an Infalling Gas Cloud:
The Lyapunov Time

Consider a star falling radially into a Schwarzschild BH

Its late-time luminosity decay is governed by the ***Lyapunov Time***

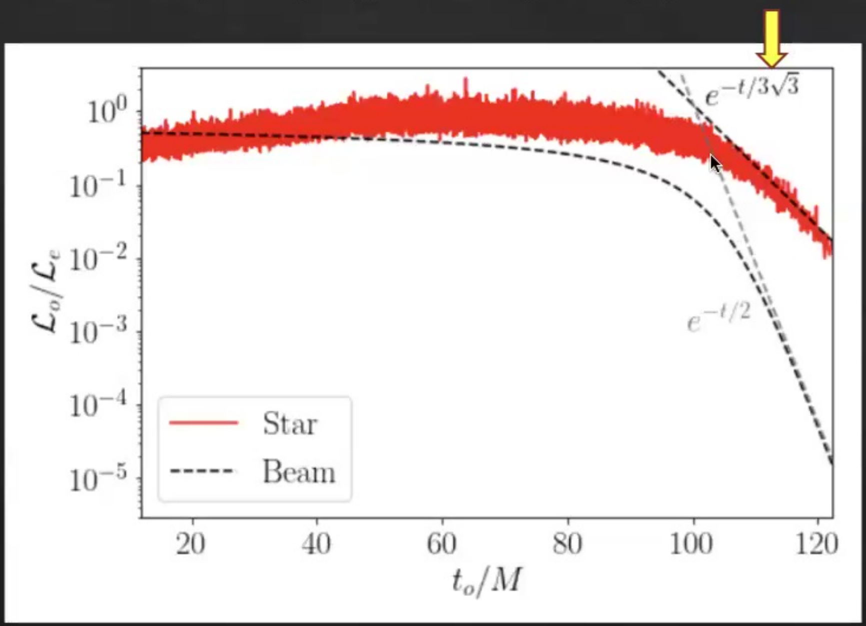

Cardoso, Duque & Foschi (2021)

This should also apply to a gas cloud falling into a BH

Moriyama, Meneshige, Honma, Akiyama (2019)

Measuring Spacetime
with Critical Parameters

$$\delta = \frac{d_{\text{sh}}}{d_{\text{sh;Schw}}} - 1 = \frac{\eta_{\text{PS}}}{\sqrt{27}M} - 1$$

$$\delta_t = \frac{t_{\ell;\text{PS}}}{t_{\ell;\text{ps;Schw}}} - 1 = \frac{t_{\ell;\text{PS}}}{\sqrt{27}M} - 1$$

$$\delta_\gamma = \frac{\gamma_{\text{PS}}}{\gamma_{\ell;\text{Schw}}} - 1 = \frac{\gamma_{\text{PS}}}{\pi} - 1$$

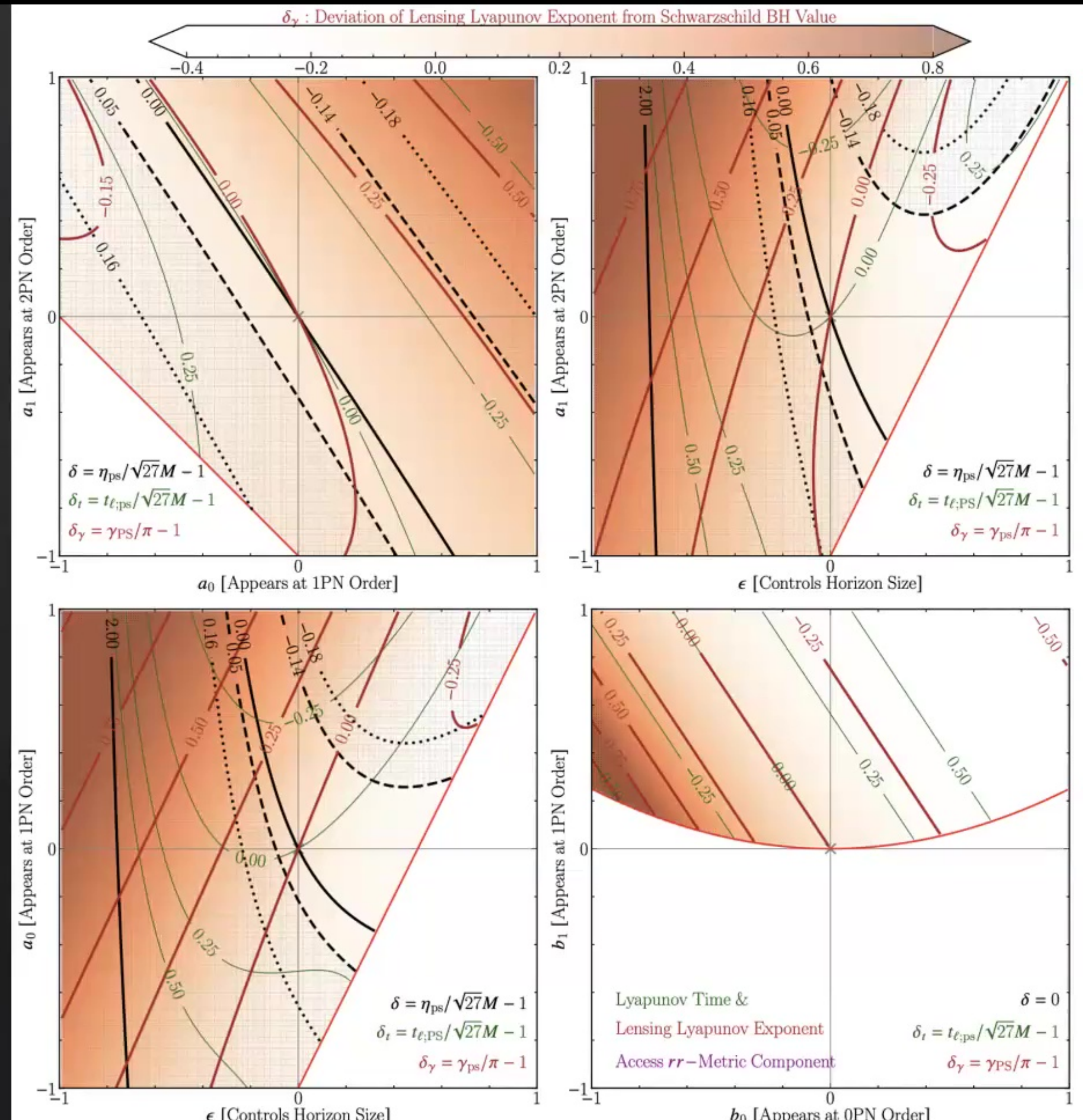

Kocherlakota et al., 2024a

Black Holes from String Theory

These black hole spacetimes contain a scalar field (dilaton), a pseudoscalar field (axion), and an electromagnetic field. Described by (M, a, D).

Sen, 1992

Metric:

$$ds^2 = g_{\alpha\beta}dx^\alpha dx^\beta = -\left(1 - \frac{2F}{\Sigma}\right)dt^2 - 2\frac{2F}{\Sigma}a\sin^2\vartheta\, dt d\varphi + \frac{\Pi}{\Sigma}\sin^2\vartheta\, d\varphi^2 + \frac{\Sigma}{\Delta}dr^2 + \Sigma\, d\vartheta^2$$

$$\begin{aligned} 2F(r) &= 2Mr \\ \Delta(r) &= r^2 - 2Mr + 2Dr + a^2 \\ \Sigma(r,\vartheta) &= r^2 + 2Dr + a^2\cos^2\vartheta \\ \Pi(r,\vartheta) &= (r^2 + 2Dr + a^2)^2 - \Delta(r)a^2\sin^2\vartheta \end{aligned}$$

[3] Chatterjee et al., 2023a

GR v.
Dilaton-Axion

$$\mathcal{L}_{\rm GR} = R - F^2$$

$$\mathcal{L}_{\rm DA} = R - e^{-2\varphi}F^2 - 2(\nabla\varphi)^2 - \frac{1}{12}e^{-4\varphi}H^2_{a\neq 0}$$

Dilaton-Axion BH: Sen (1992) solution

Nonspinning Limit:
Dilaton/GMGHS BH: Gibbons & Maeda (1988); Garfinkle, Horowitz & Strominger (1991)

*In our simulations, accreting matter "feels" *only* the spacetime geometry.

Spinning Stringy "Dilaton-Axion" Black Holes

Magnetically-Arrested Disk (MAD) simulations

Chatterjee et al., 2023a

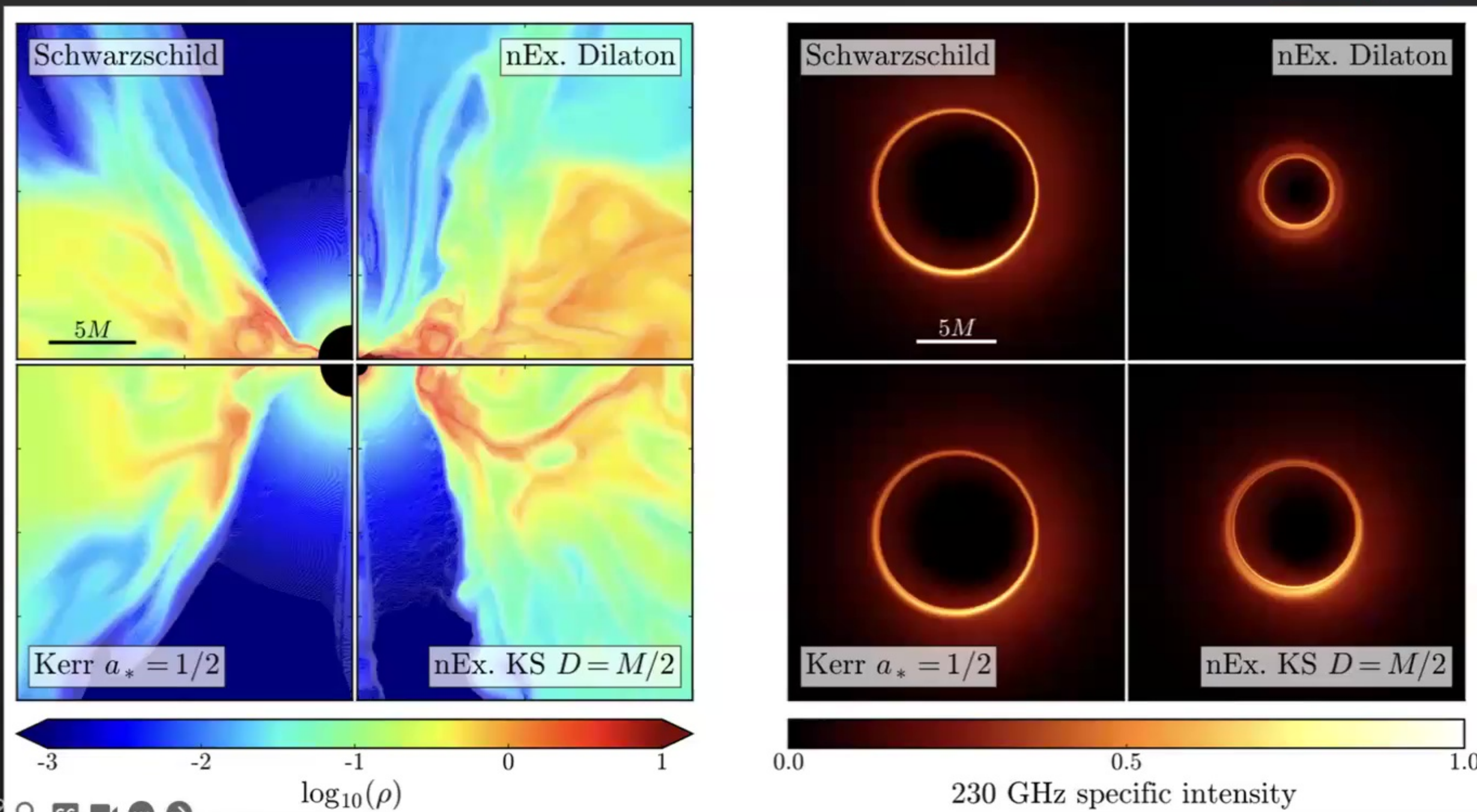

Nonspinning:

Mizuno et al. (2018)
Fromm et al. (2022)
Röder et al. (2023)

We *can* tell the difference between black holes from GR and String Theory!

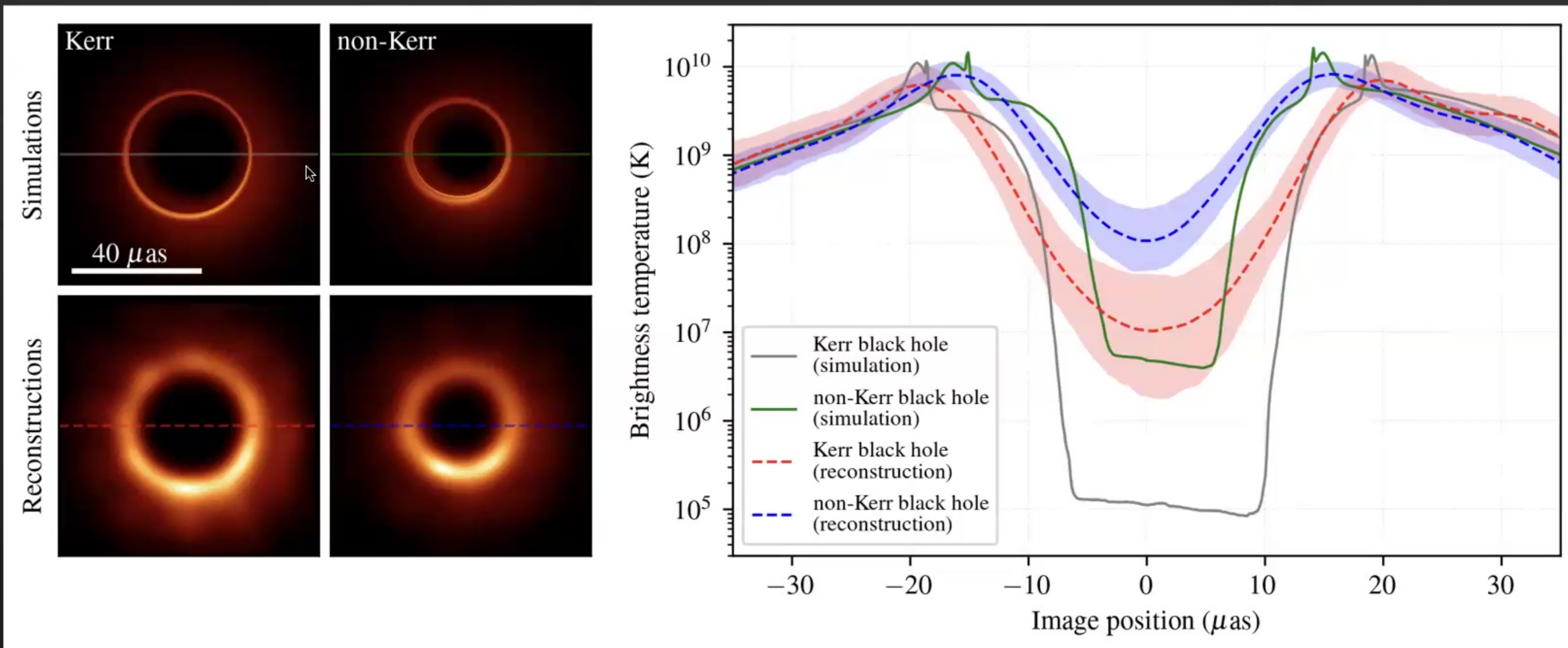

Thanks to Paul Tiede and Dom Pesce (Center for Astrophysics) for reconstructions

Johannsen-Psaltis
Parametrized BHs

alpha_13 tunes the size of the shadow

alpha_22 tunes the quadrupole moment

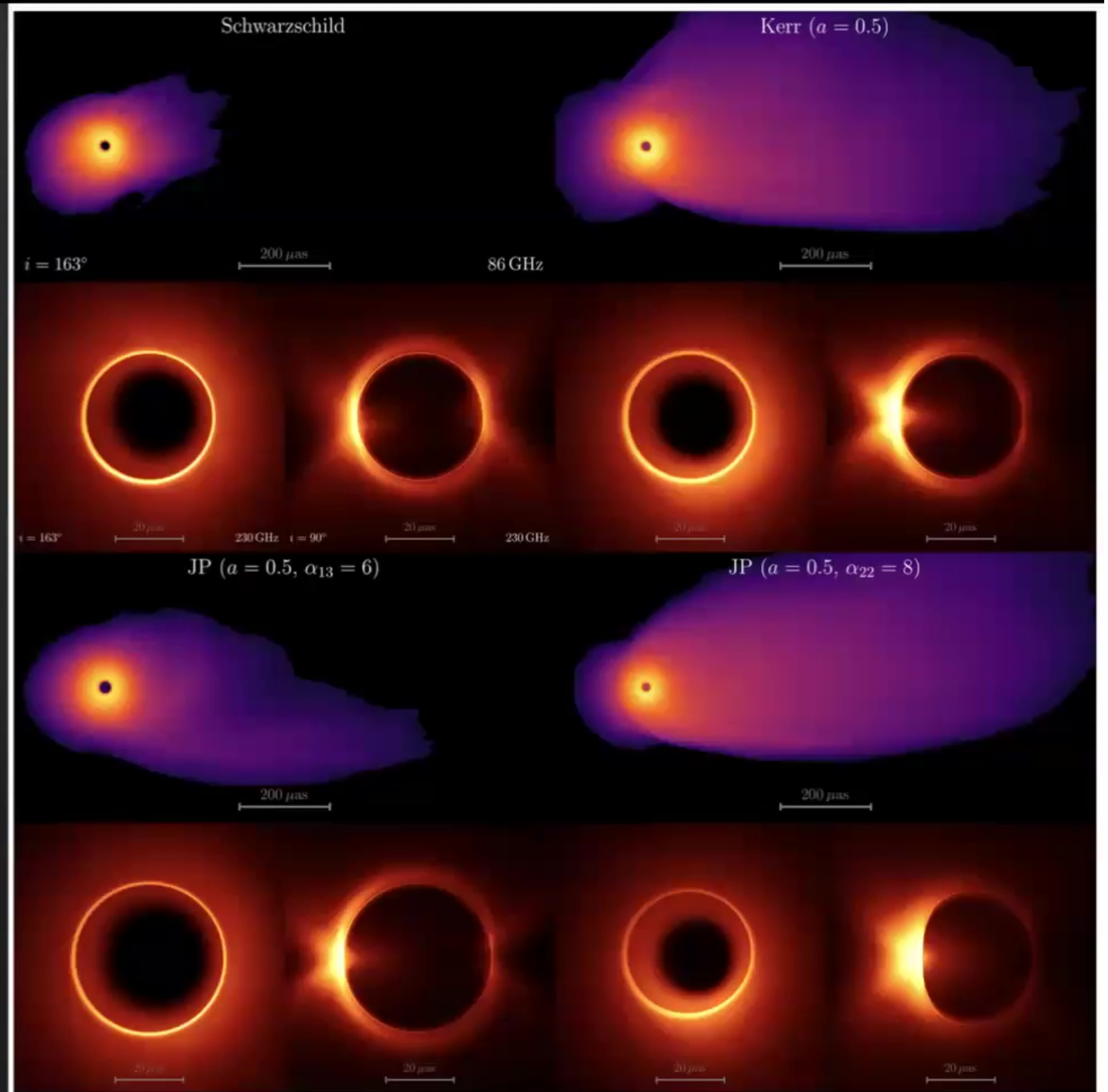

Chatterjee et al., 2023b

Outline

[I] Measuring spacetime using black hole (BH) imaging: Current Status & Future Prospects

Kocherlakota et al., 2024 a, b

Chatterjee et al., 2023 a,b

[II] Observable differences between simulated images of Kerr and non-Kerr BHs

[III] What sets the jet power of a non-Kerr BH?

Jets powered by Kerr BHs: The Blandford-Znajek Mechanism

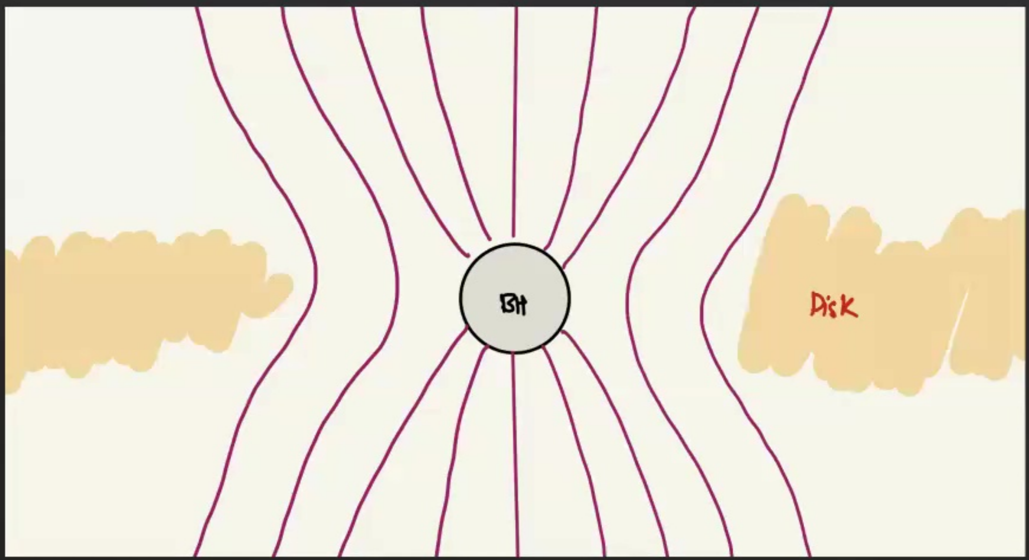

$$P_{\rm jet} \sim a^2 \cdot B^2 \cdot r_{\rm g}^2 \cdot c$$

Blandford and Znajek, 1977

Jets powered by Kerr BHs: The Blandford-Znajek Mechanism

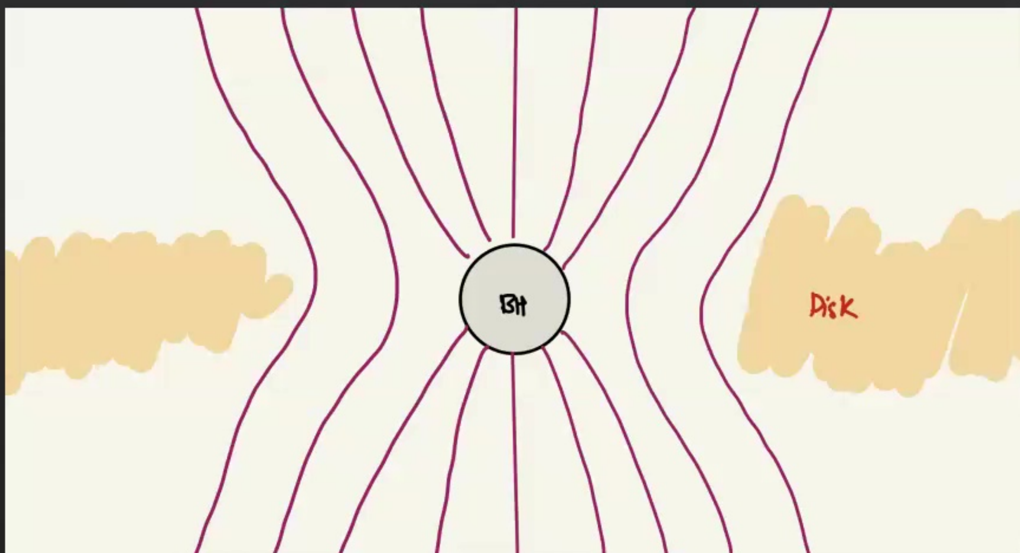

$$P_{\rm jet} \sim a^2 \cdot B^2 \cdot r_{\rm g}^2 \cdot c$$

$$P_{\rm jet} \propto \Phi^2 (a/r_{\rm g})^2$$

$$\Phi \sim B \cdot r_{\rm g}^2$$ ***Horizon Magnetic Flux***

Blandford and Znajek, 1977

Jets powered by Kerr BHs: The Blandford-Znajek Mechanism

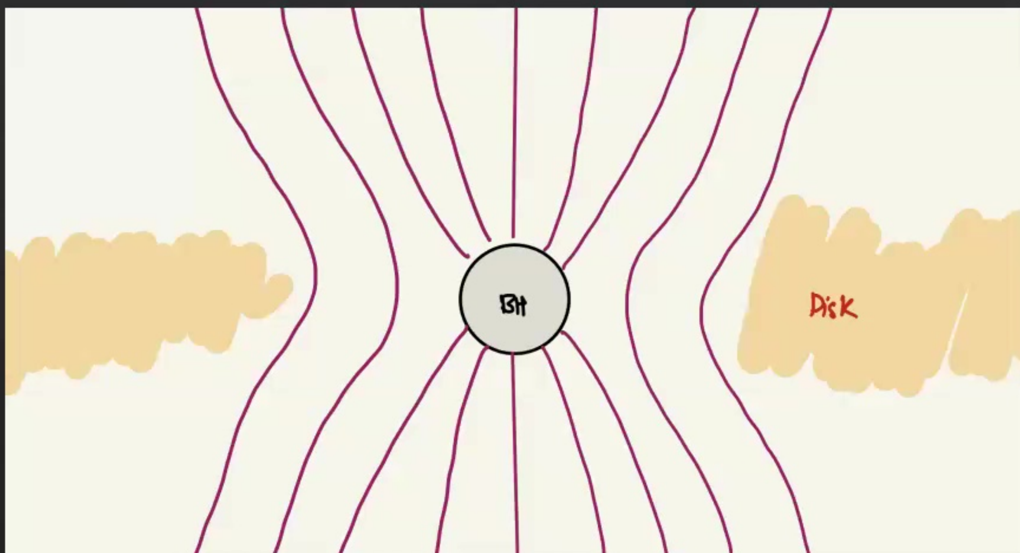

$$P_{\rm jet} \sim a^2 \cdot B^2 \cdot r_{\rm g}^2 \cdot c$$

Better beyond a>0.5

$$P_{\rm jet} \propto \Phi^2 (a/r_{\rm g})^2$$

$$P_{\rm jet} \propto \Phi^2 \Omega_{\rm H}^2$$

$$\Phi \sim B \cdot r_{\rm g}^2$$

Horizon Magnetic Flux

Blandford and Znajek, 1977

Tchekhovskoy, Narayan, McKinney, 2010

Horizon Magnetic Flux

$$P_{\text{jet}} \propto \Phi^2 \Omega_{\text{H}}^2$$

Minimum power: 0 [Nonspinning BH]

Max. power is order of the rest-mass accretion rate

$$P_{\text{jet;Max}} \sim \dot{M}c^2 \propto \Phi_{\text{Max}}^2 \Omega_{\text{H}}^2$$

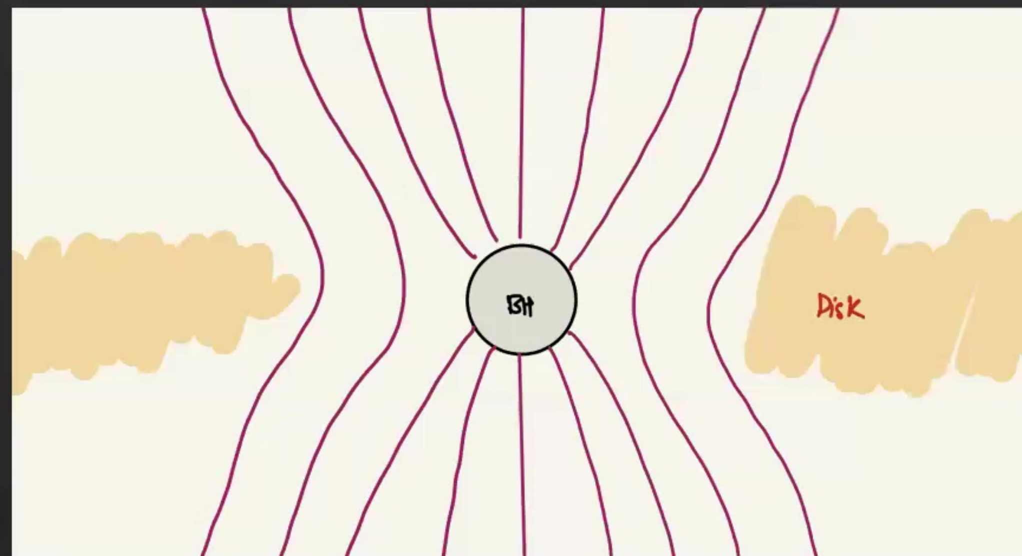

Jet efficiency

$$\eta_{\text{jet}} := \frac{P_{\text{jet}}}{\dot{M}c^2}$$

Horizon Magnetic Flux

$$P_{\rm jet} \propto \Phi^2 \Omega_{\rm H}^2$$

Minimum power: 0 [Nonspinning BH]

Max. power is order of the rest-mass accretion rate

$$P_{\rm jet;Max} \sim \dot{M}c^2 \propto \Phi_{\rm Max}^2 \Omega_{\rm H}^2$$

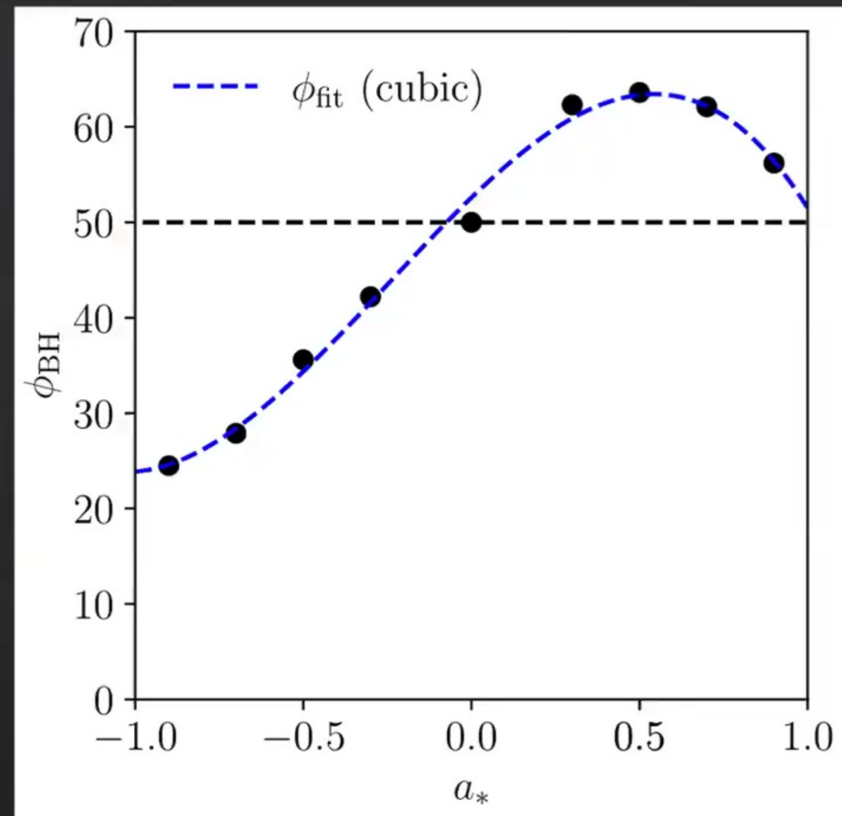

Jet efficiency

$$\eta_{\rm jet} := \frac{P_{\rm jet}}{\dot{M}c^2}$$

Max Jet efficiency

$$\eta := \frac{P_{\rm jet;Max}}{\dot{M}c^2} \propto \frac{\Phi_{\rm Max}^2 \Omega_{\rm H}^2}{\dot{M}c^2} \propto \phi_{\rm H}^2 \Omega_{\rm H}^2$$

Narayan et al., 2022

Universality of Energy Extraction

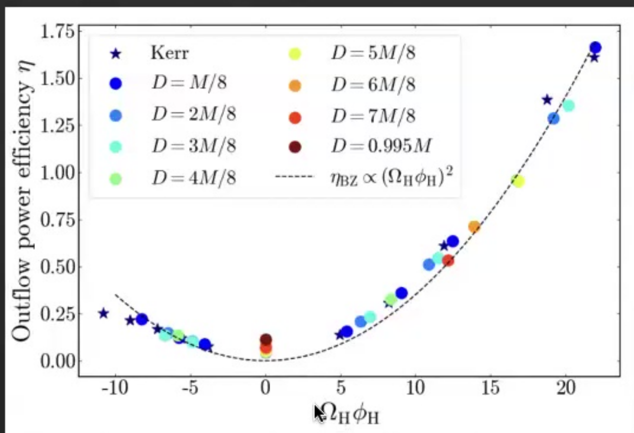

"Stringy" Black Holes

Non-Kerr BHs obey the same trend!

Chatterjee et al., 2023a

Johannsen-Psaltis Black Holes

Chatterjee et al., 2023b

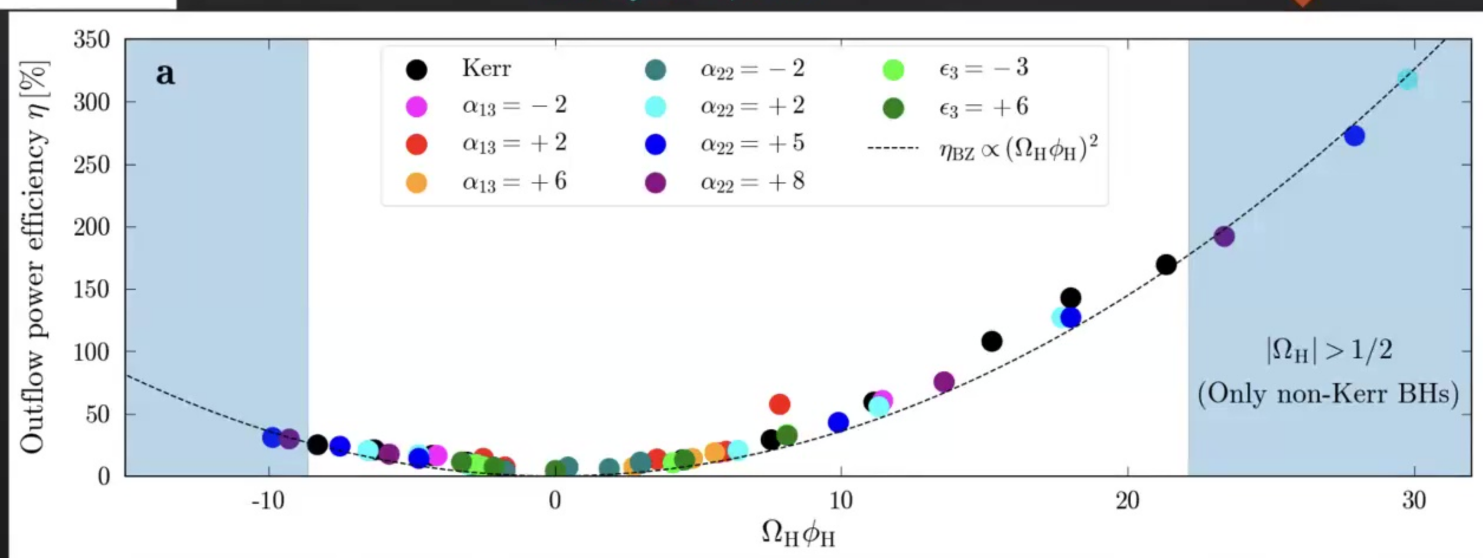

Conclusions

- Critical Parameters may become accessible with the next generation of black hole (BH) imaging
  The Delay Time, the Lensing Lyapunov Exponent, and the Lyapunov Time
- These can set up new and stringent tests of the spacetime as well as of general relativity (GR)
- The n=1 ring width also imposes nontrivial constraints on spacetime
- Simulations in spinning non-Kerr spacetimes are now becoming possible
- We have used these to show that we can distinguish between different BHs
- We have studied the energetics of jets in 100 different BH spacetimes and discover universal behaviour:
  The Blandford-Znajek mechanism operates in all BH spacetimes

Thanks!

Conclusions

- Critical Parameters may become accessible with the next generation of black hole (BH) imaging
  The Delay Time, the Lensing Lyapunov Exponent, and the Lyapunov Time
- These can set up new and stringent tests of the spacetime as well as of general relativity (GR)
- The n=1 ring width also imposes nontrivial constraints on spacetime
- Simulations in spinning non-Kerr spacetimes are now becoming possible
- We have used these to show that we can distinguish between different BHs
- We have studied the energetics of jets in 100 different BH spacetimes and discover universal behaviour:
  The Blandford-Znajek mechanism operates in all BH spacetimes

Thanks!